

Highly Multiplexed Immunofluorescence of the Human Kidney using Co-Detection by Indexing (CODEX)

Elizabeth K. Neumann^{1,2}, N. Heath Patterson^{1,2}, Emilio S. Rivera^{1,2}, Jamie L. Allen^{1,2}, Maya Brewer³, Mark P. deCaestecker³, Richard M. Caprioli^{1,2,6}, Agnes B. Fogo^{3,4,5} and Jeffrey M. Spraggins^{2,6,7}

¹Department of Biochemistry, Vanderbilt University, Nashville, TN, USA 37232

²Mass Spectrometry Research Center, Vanderbilt University, Nashville, TN, USA 37232.

³Division of Nephrology and Hypertension, Department of Medicine, Vanderbilt University Medical Center, Nashville, TN USA 37232

⁴Department of Pathology, Microbiology and Immunology, Vanderbilt University Medical Center, Nashville, TN USA 37232.

⁵Departments of Medicine and Pediatrics, Vanderbilt University Medical Center, Nashville, TN, USA 37232

⁶Department of Chemistry, Vanderbilt University, Nashville, TN, USA 37232

⁷Department of Cell and Developmental Biology, Vanderbilt University School of Medicine, Nashville, TN, USA 37232

SUPPORTING INFORMATION

Table of Contents

Figure S1	Fluorescence Histograms for Each CODEX Fluorescence Cycle.....	S-3
Figure S2	Comparison between Indirect IF and CODEX Conjugated Antibodies.....	S-4
Figure S3	DAPI Images Through Each Cycle Region 1	S-5
Figure S4	DAPI Images Through Each Cycle Region 2	S-6
Figure S5	DAPI Images Through Each Cycle Region 3	S-7
Figure S6	CODEX IF Image of Third Patient.....	S-8
Figure S7	CODEX IF Image of Second Patient	S-9
Figure S8	Full Resolution Fluorescence Image of PAS Histological Stain	S-10
Figure S9	Full Resolution Fluorescence Image of α -Smooth Muscle Actin.....	S-11
Figure S10	Full Resolution Fluorescence Image of Aquaporin 1	S-12
Figure S11	Full Resolution Fluorescence Image of Aquaporin 2.....	S-13
Figure S12	Full Resolution Fluorescence Image of β -Catenin.....	S-14
Figure S13	Full Resolution Fluorescence Image of Calbindin	S-15

Figure S14	Full Resolution Fluorescence Image of CD7.....	S-16
Figure S15	Full Resolution Fluorescence Image of CD31.....	S-17
Figure S16	Full Resolution Fluorescence Image of CD38.....	S-18
Figure S17	Full Resolution Fluorescence Image of CD45.....	S-19
Figure S18	Full Resolution Fluorescence Image of CD90.....	S-20
Figure S19	Full Resolution Fluorescence Image of CD93.....	S-21
Figure S20	Full Resolution Fluorescence Image of Cytokeratin 7.....	S-22
Figure S21	Full Resolution Fluorescence Image of DAPI.....	S-23
Figure S22	Full Resolution Fluorescence Image of E-Cadherin	S-24
Figure S23	Full Resolution Fluorescence Image of KDR/VegF	S-25
Figure S24	Full Resolution Fluorescence Image of Laminin	S-26
Figure S25	Full Resolution Fluorescence Image of MARCKS.....	S-27
Figure S26	Full Resolution Fluorescence Image of Nestin	S-28
Figure S27	Full Resolution Fluorescence Image of PARP1.....	S-29
Figure S28	Full Resolution Fluorescence Image of Renin.....	S-30
Figure S29	Full Resolution Fluorescence Image of Tryptase.....	S-31
Figure S30	Full Resolution Fluorescence Image of Uromodulin	S-32
Figure S31	Full Resolution Fluorescence Image of Vimentin.....	S-33
Figure S32	Fluorescence Images of FFPE Tissue	S-34
Figure S33	Expanded Glomeruli Fluorescence Images	S-35
Figure S34	CODEX IF of Diabetic Nephropathy Patient 1	S-36
Figure S35	CODEX IF of Diabetic Nephropathy Patient 2	S-38
Figure S36	CODEX IF of Diabetic Nephropathy Patient 3	S-40
Extended Methods.....		S-42

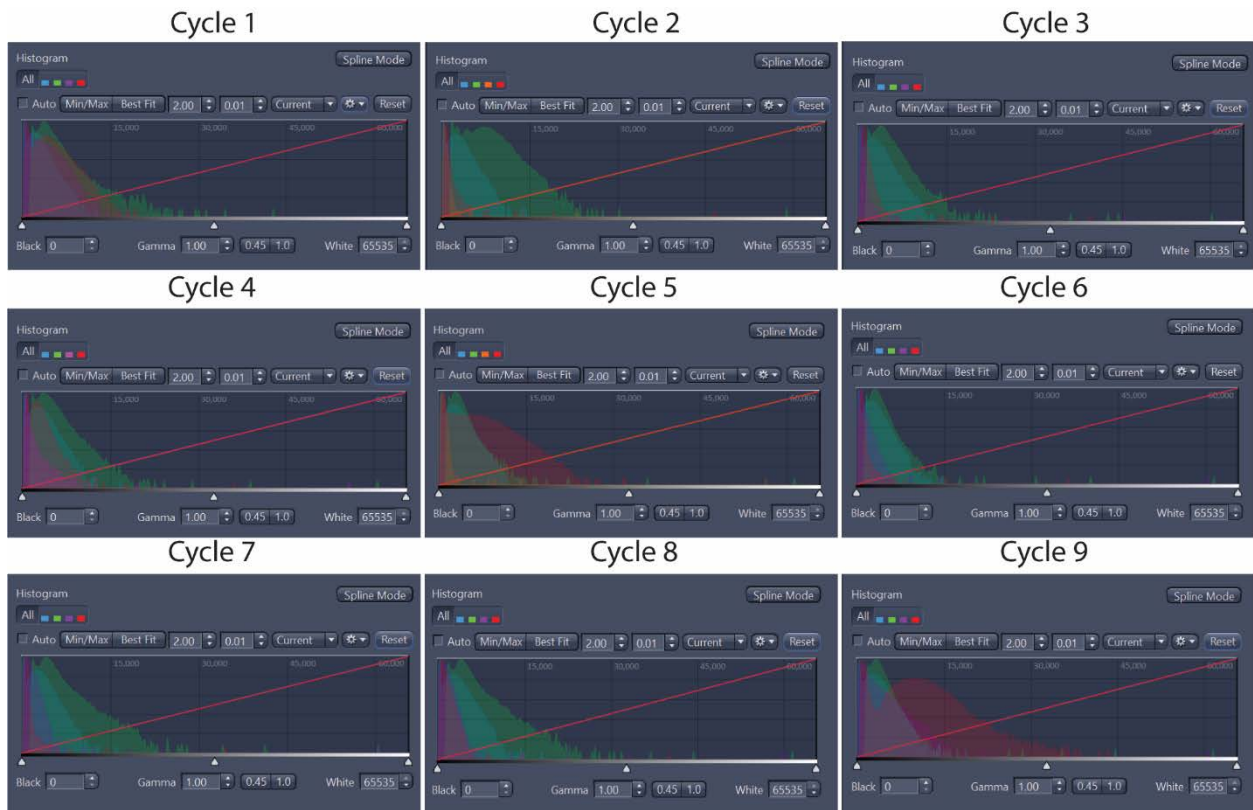


Figure S1: Fluorescence histograms for each CODEX cycle.

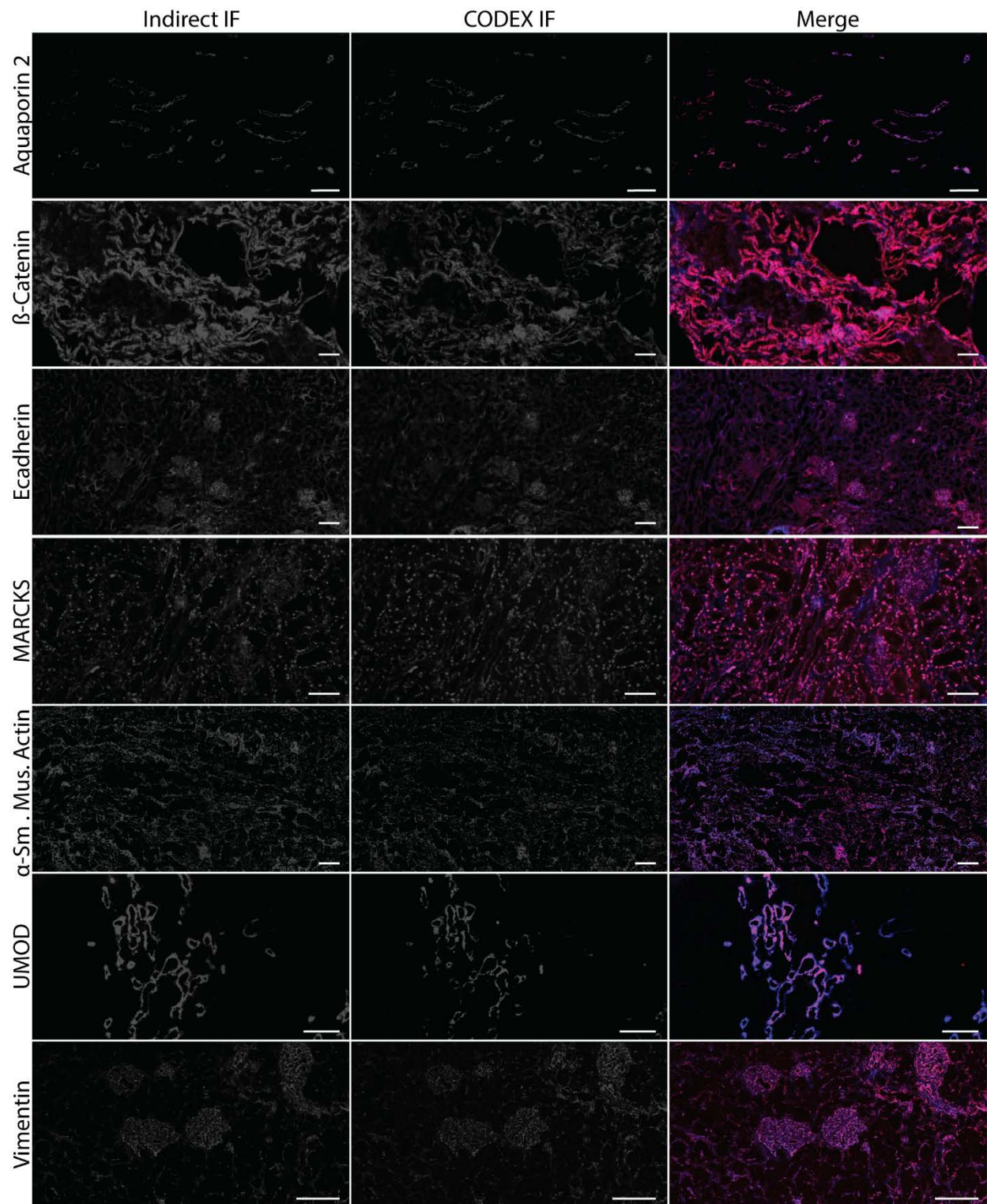


Figure S2: Comparison of indirect IF versus CODEX conjugated antibodies using the same primary antibody. Overlaid images show high concordance between the indirect IF and CODEX IF. Scale bars 250 μ m.

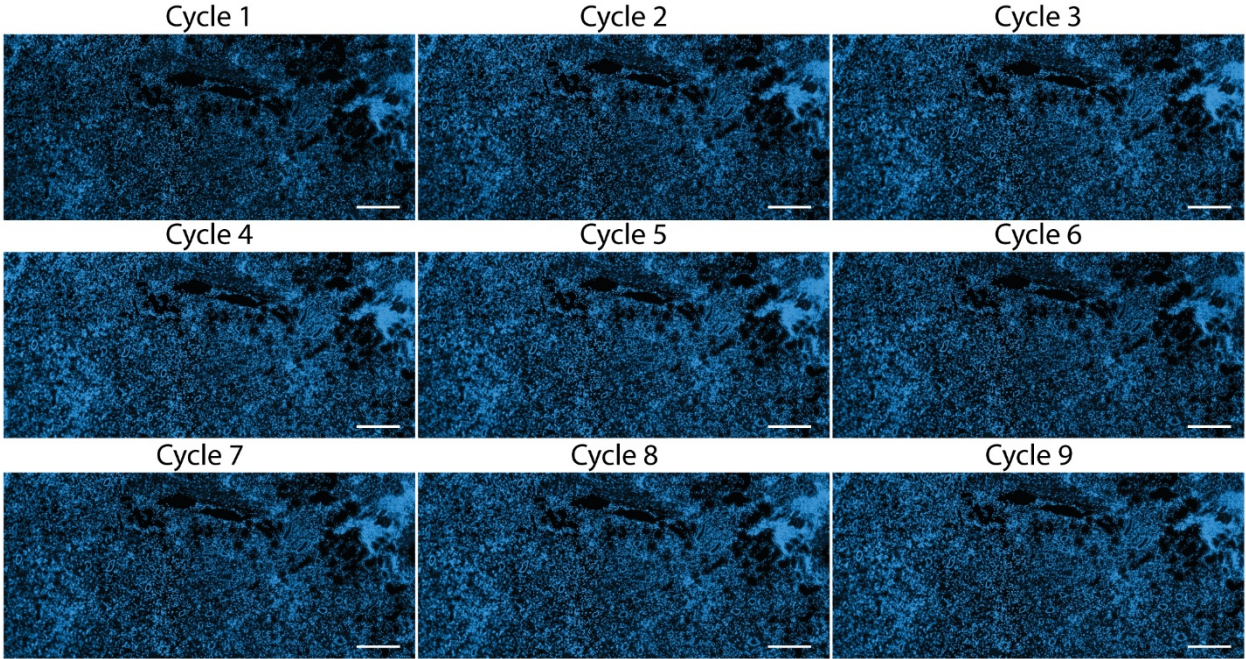


Figure S3: Fluorescence images of DAPI throughout each cycle at one location of the tissue. Scale bars are 500 μm .

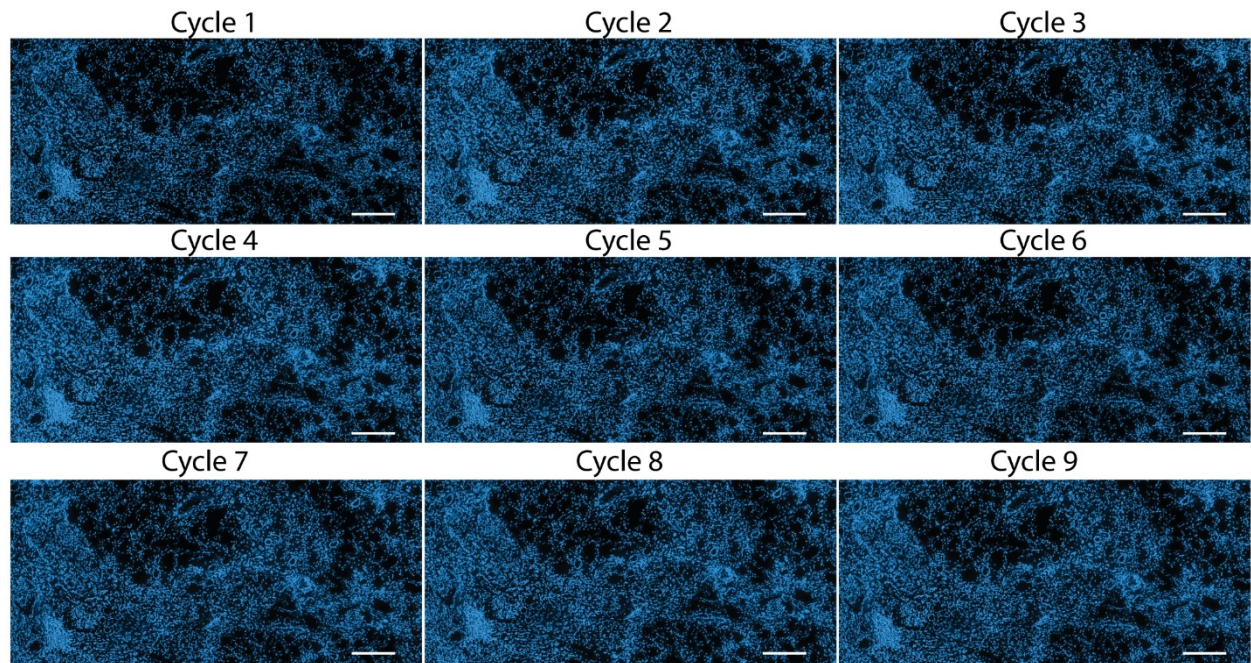


Figure S4: Fluorescence images of DAPI throughout each cycle at a second location of the tissue. Scale bars are 500 μm .

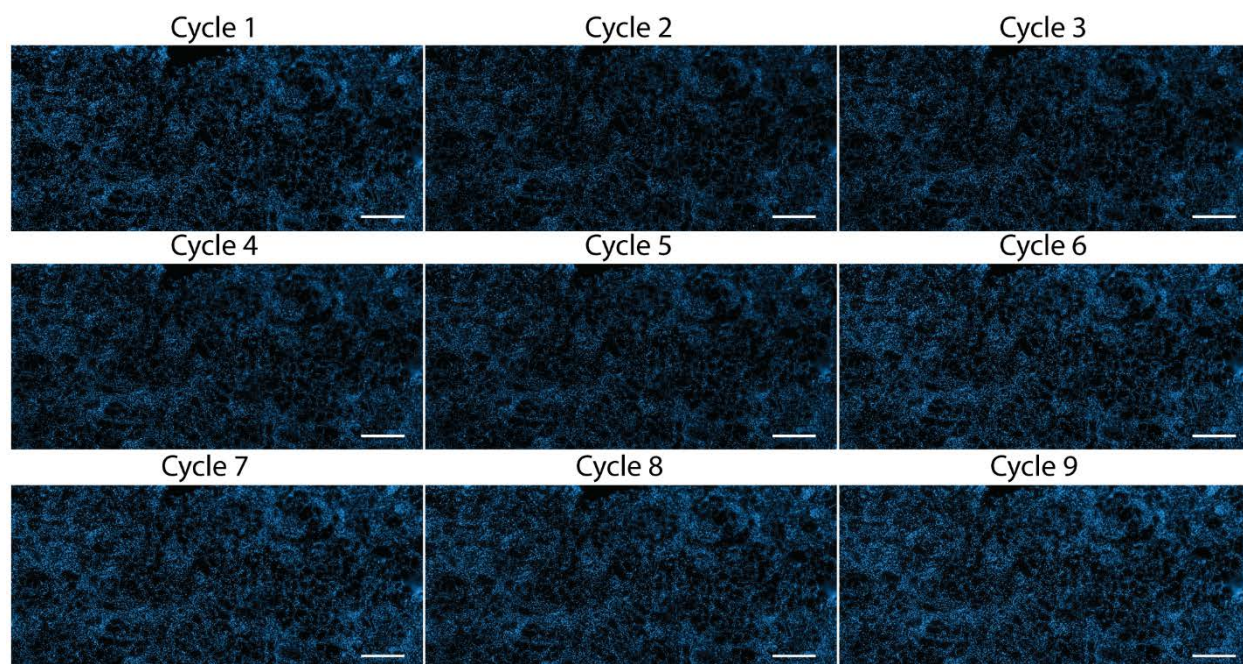


Figure S5: Fluorescence images of DAPI throughout each cycle at a third location of the tissue. Scale bars are 500 μm .

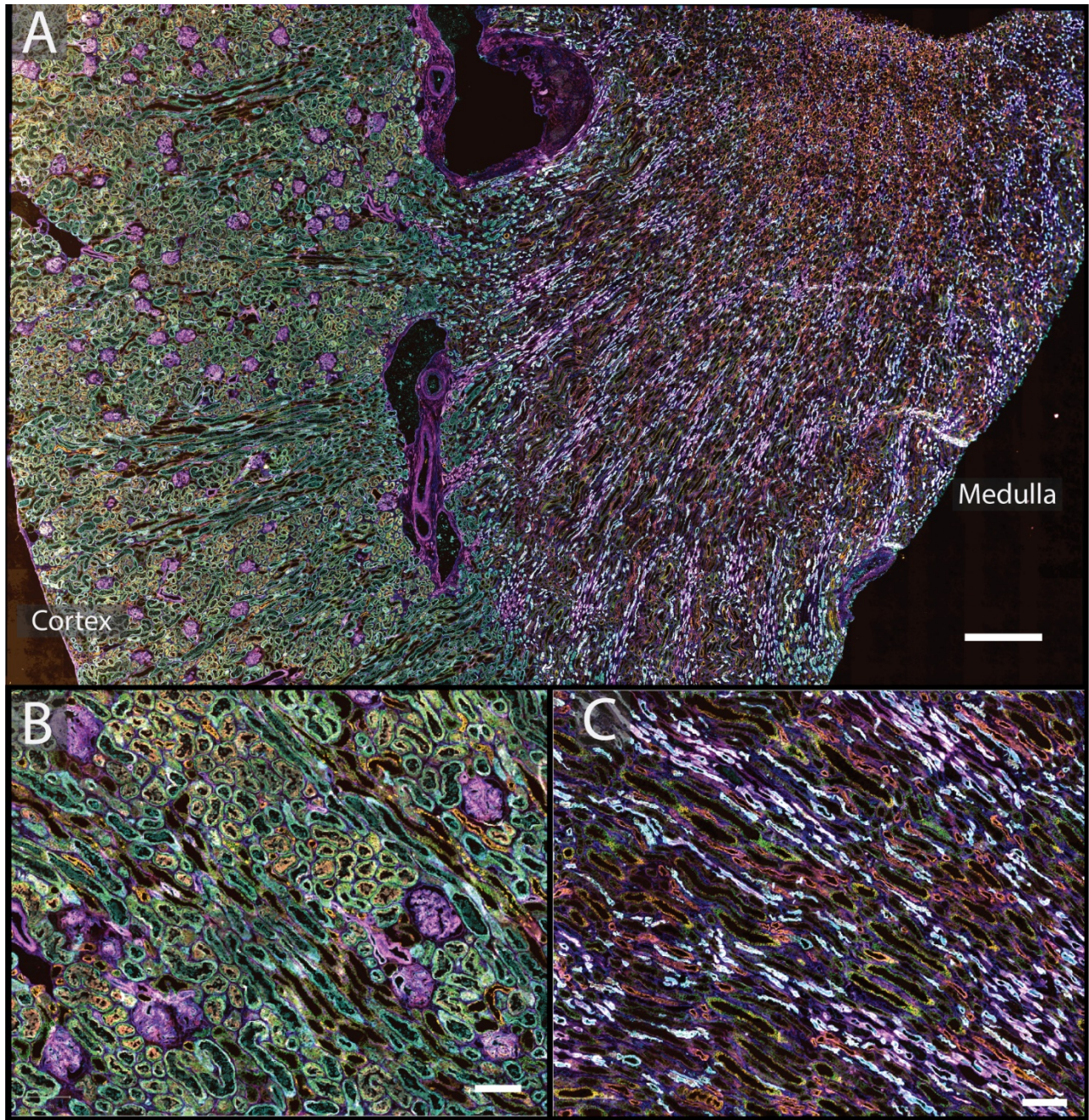


Figure S6: CODEX multiplexed immunofluorescence of kidney section for a 44-year-old male using cytokeratin 7 (pink), α -smooth muscle actin (red), tryptase (orange), nestin (yellow), β -catenin (green), aquaporin 1 (teal), vimentin (dark blue). Scale bars are 1 mm for panel A and 200 μ m for panels B-C.

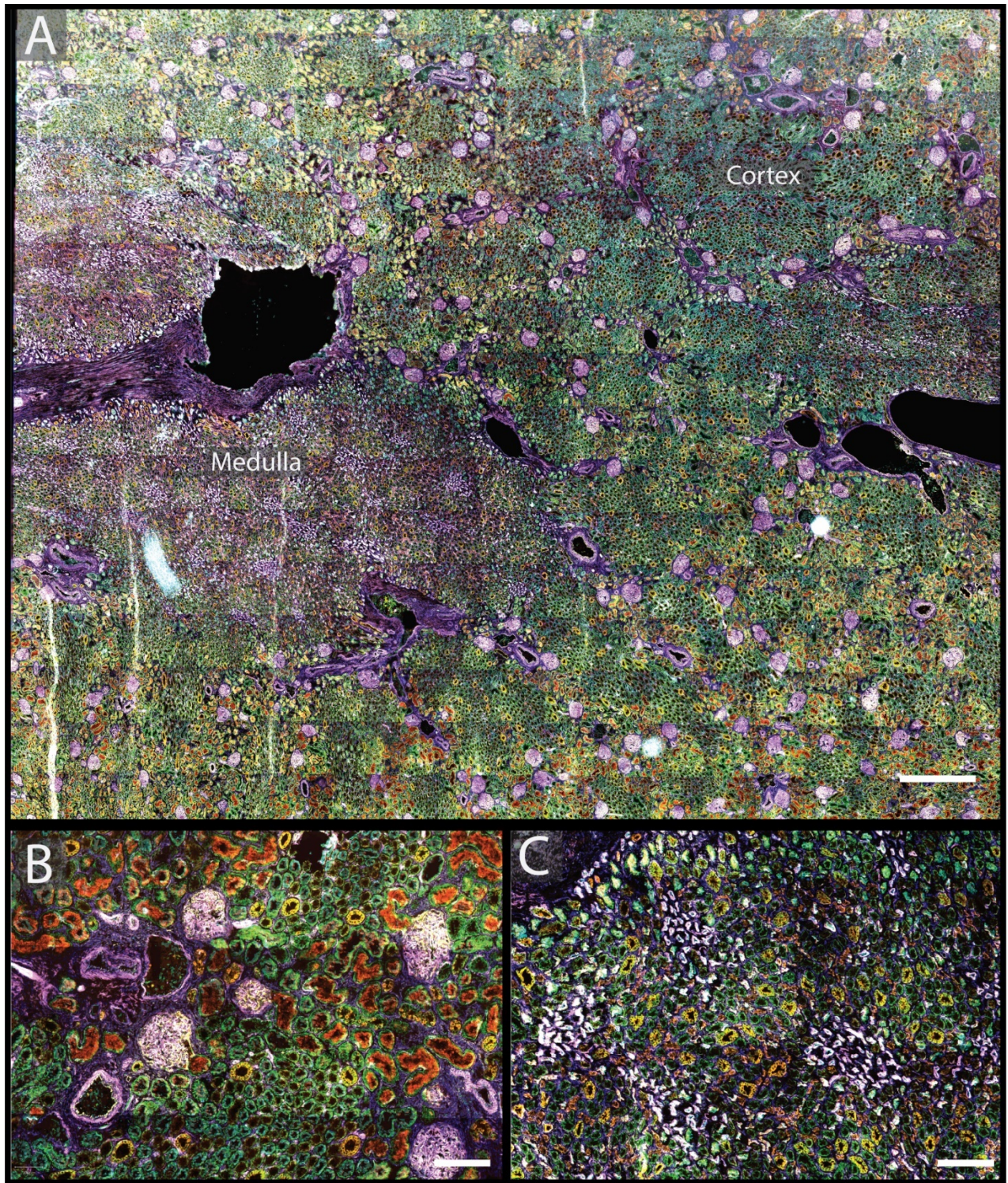


Figure S7: CODEX multiplexed immunofluorescence of kidney section for a 77-year-old female using cytokeratin 7 (pink), α -smooth muscle actin (red), tryptase (orange), nestin (yellow), β -catenin (green), aquaporin 1 (teal), vimentin (dark blue). Scale bars are 1 mm for panel A and 200 μ m for panels B-C.



Figure S8: Serial histological periodic acid Schiff stain for the tissue from Figure 1 in the main text. Scale bar is 1 mm.

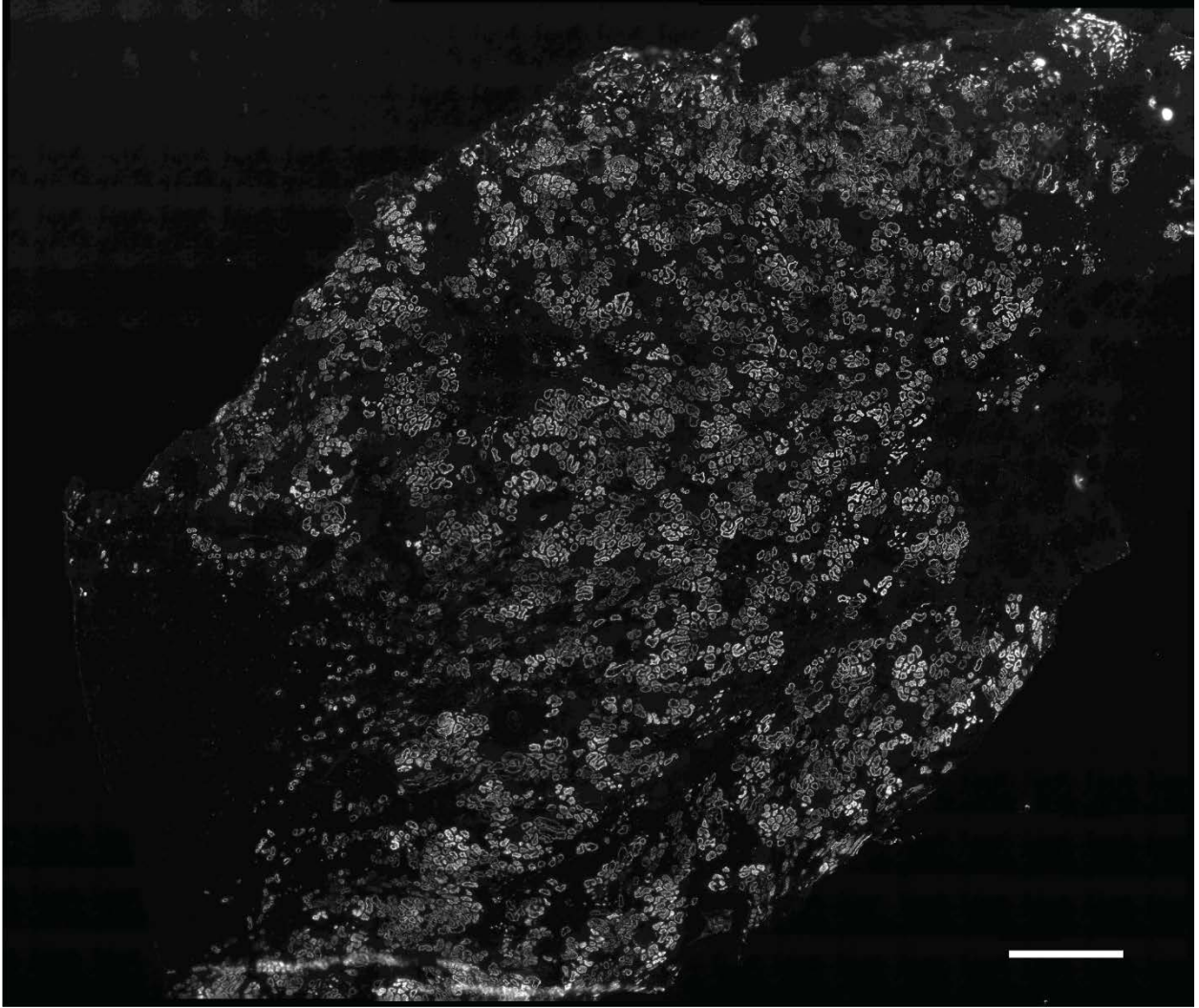


Figure S9: Single channel image of α -smooth muscle actin. Scale bar is 1 mm.

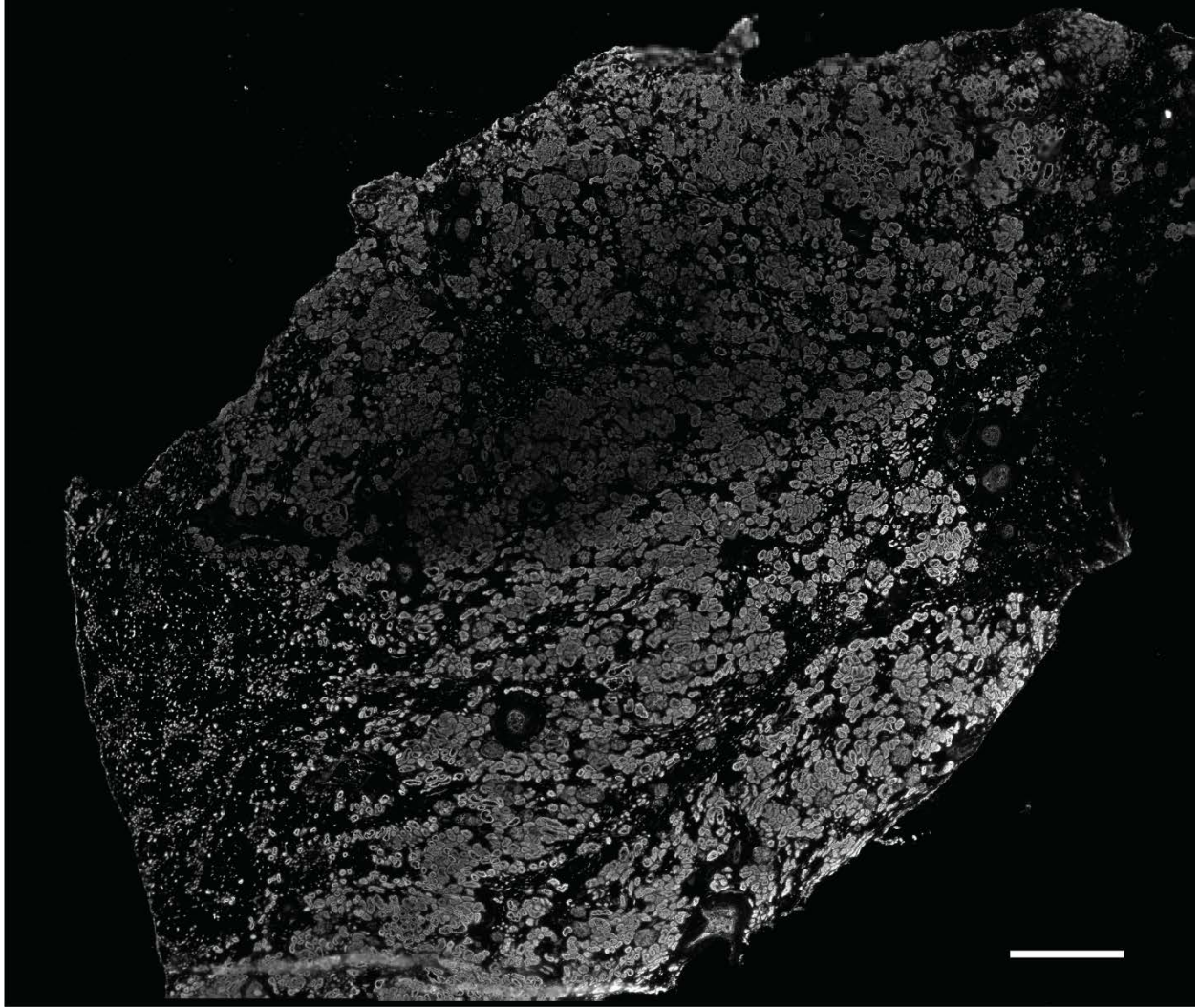


Figure S10: Single channel image of aquaporin 1. Scale bar is 1 mm.

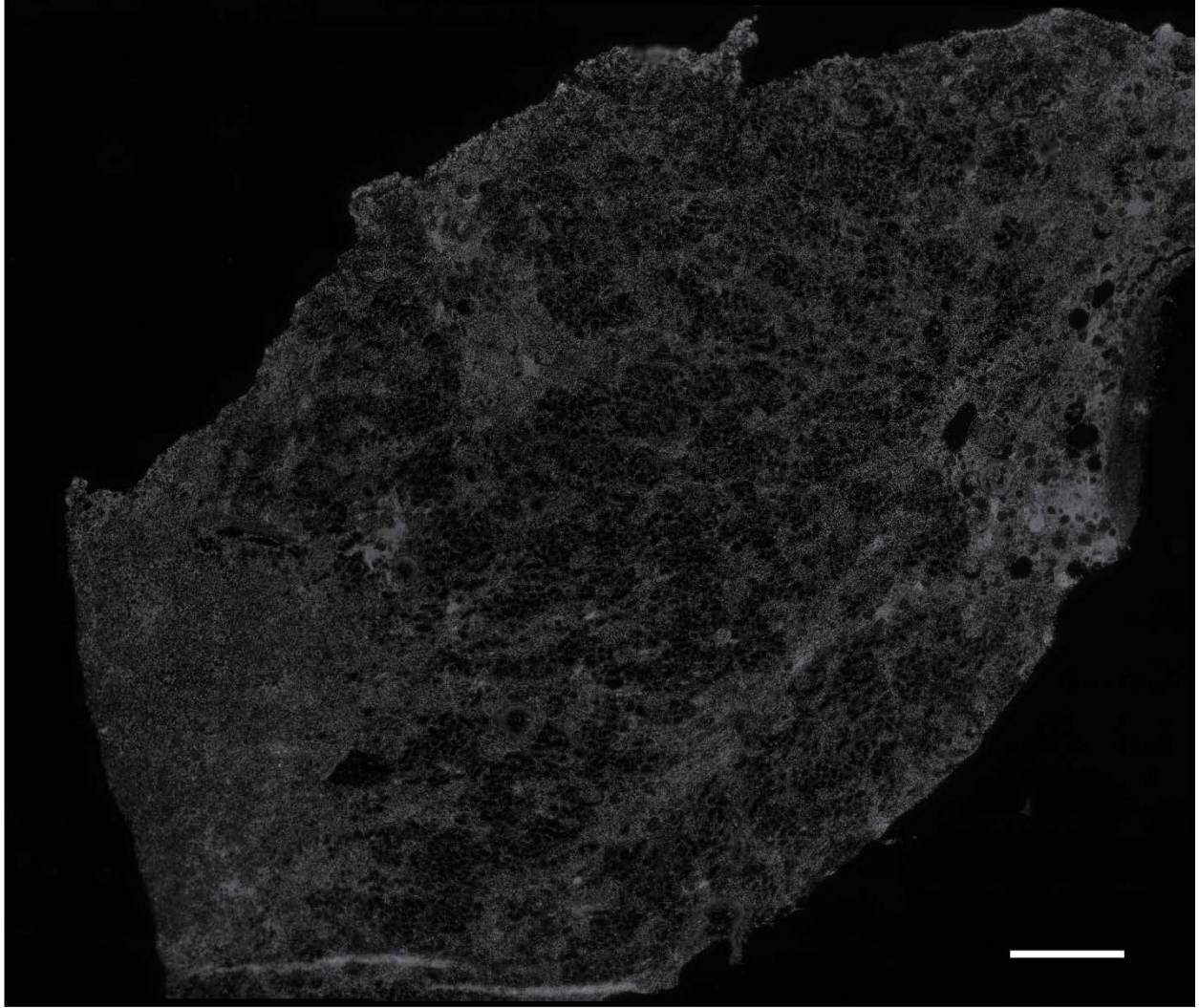


Figure S11: Single channel image of aquaporin 2. Scale bar is 1 mm.

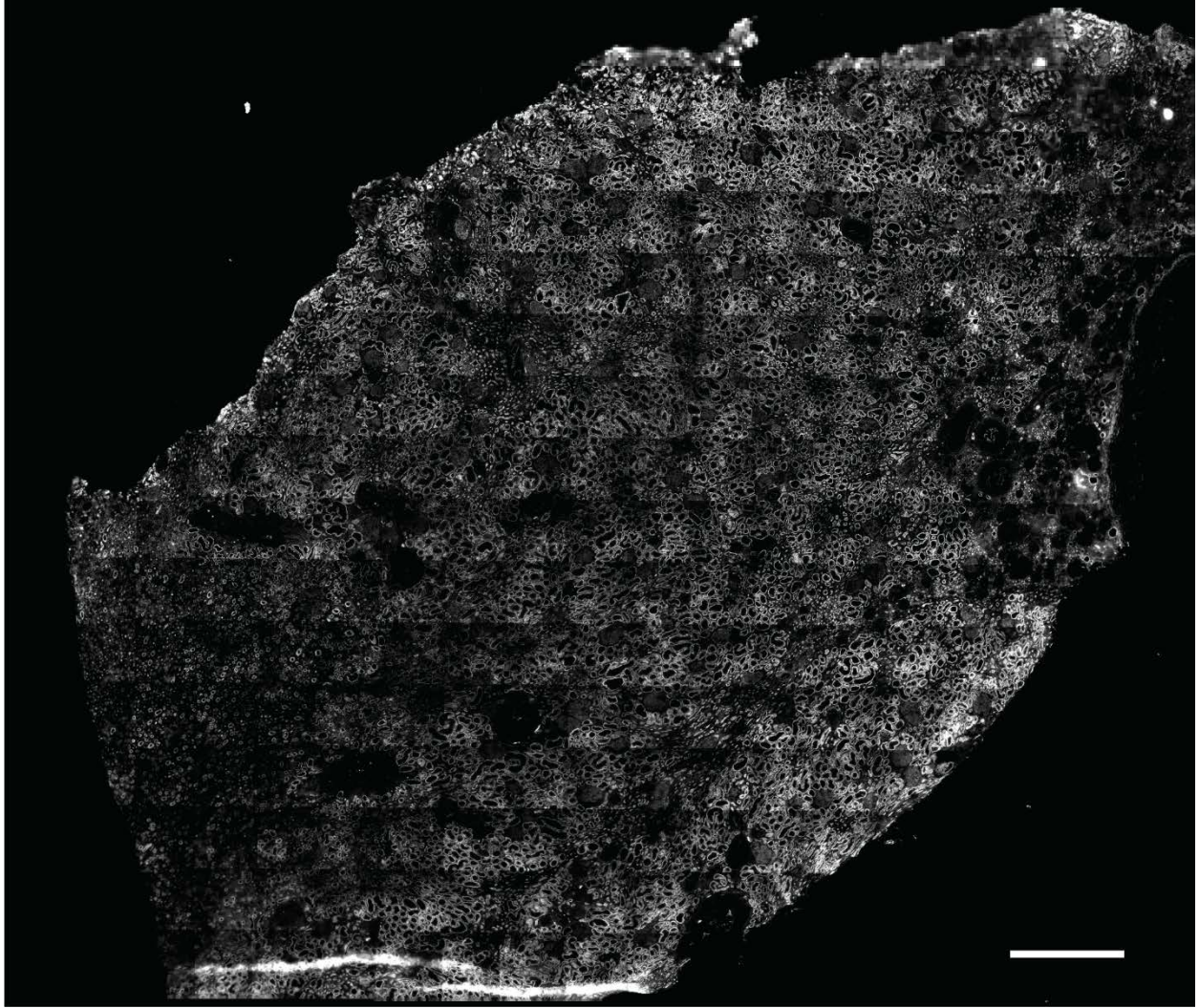


Figure S12: Single channel image of β -catenin. Scale bar is 1 mm.

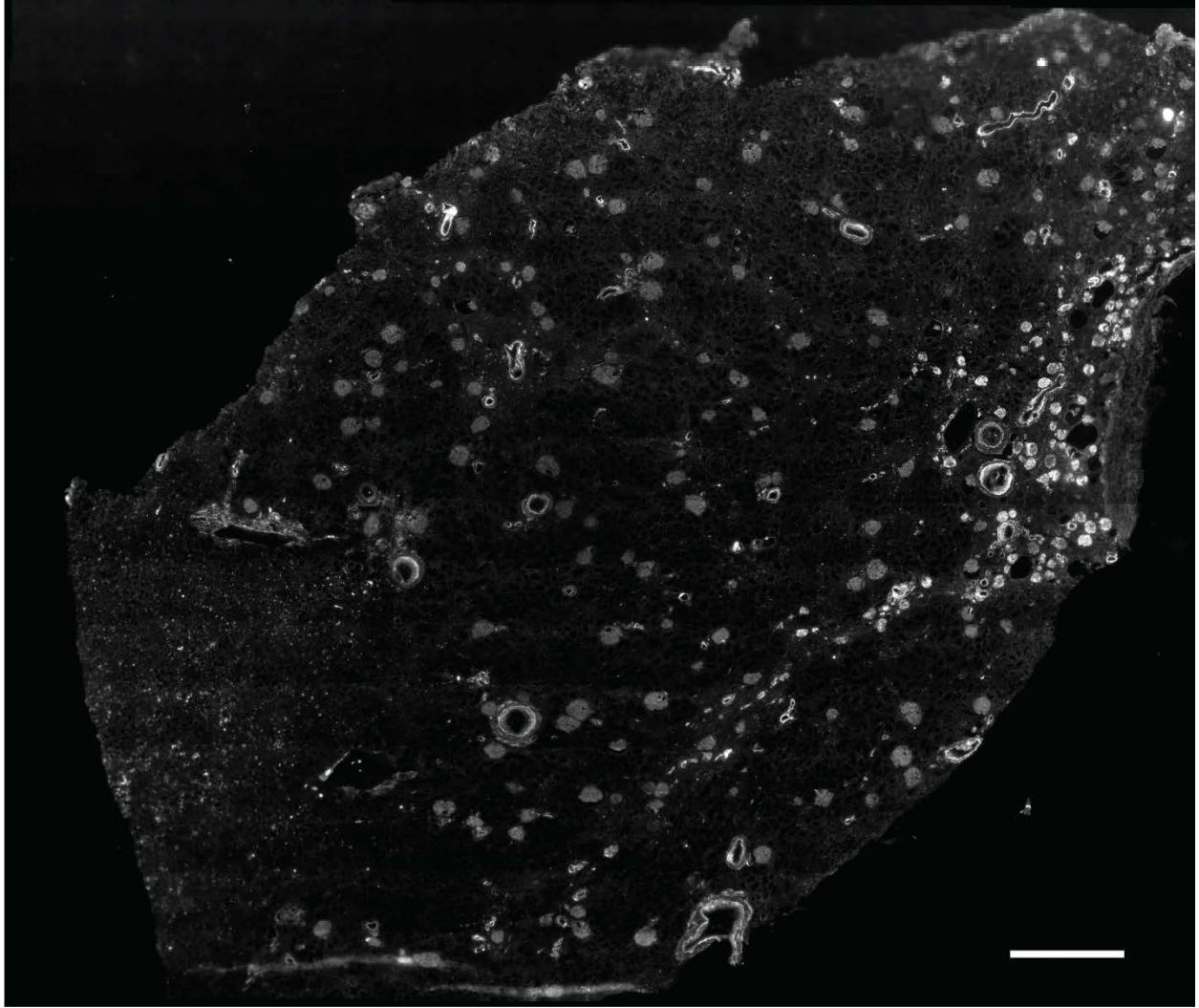


Figure S13: Single channel image of calbindin. Scale bar is 1 mm.

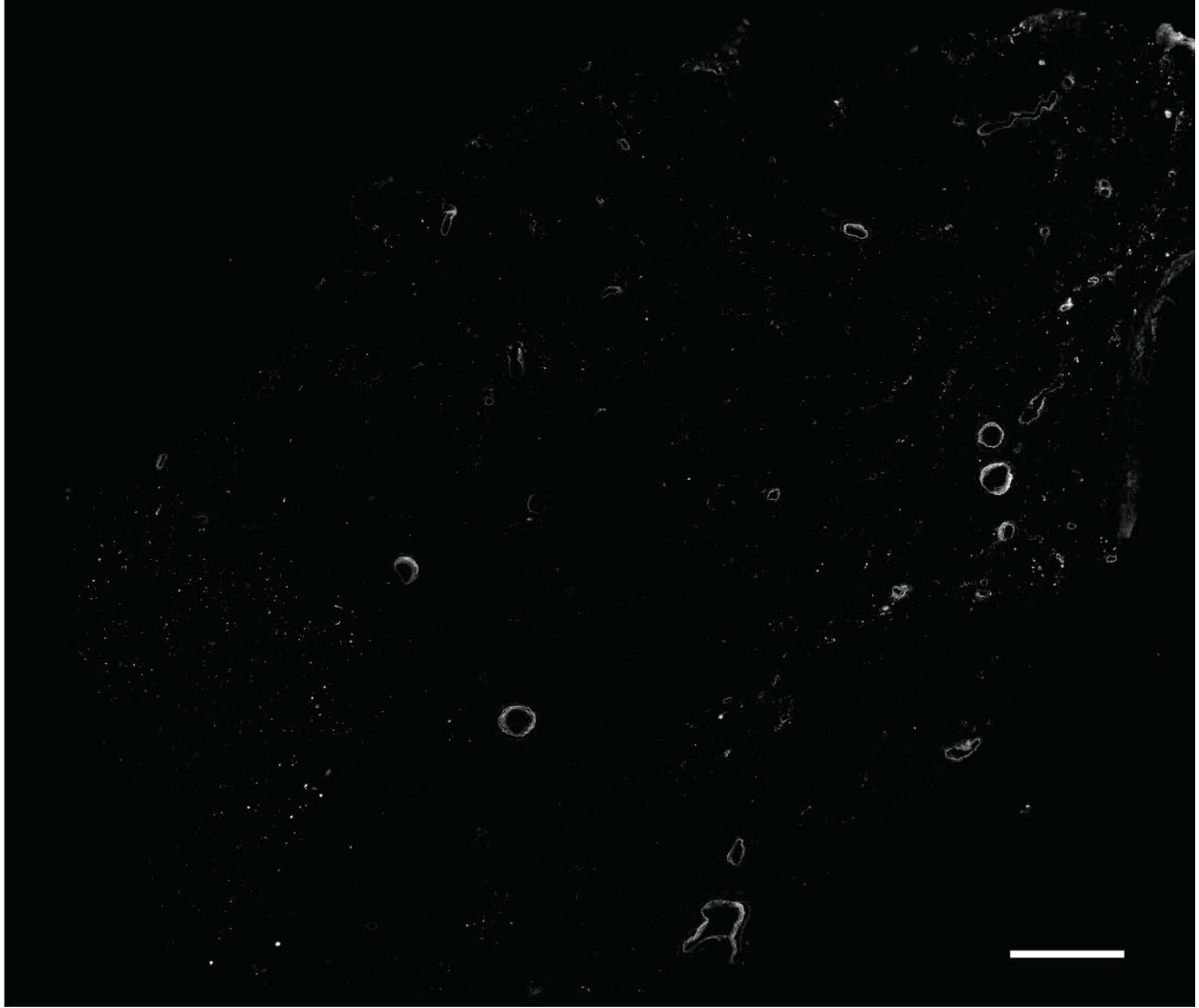


Figure S14: Single channel image of CD7. Scale bar is 1 mm.

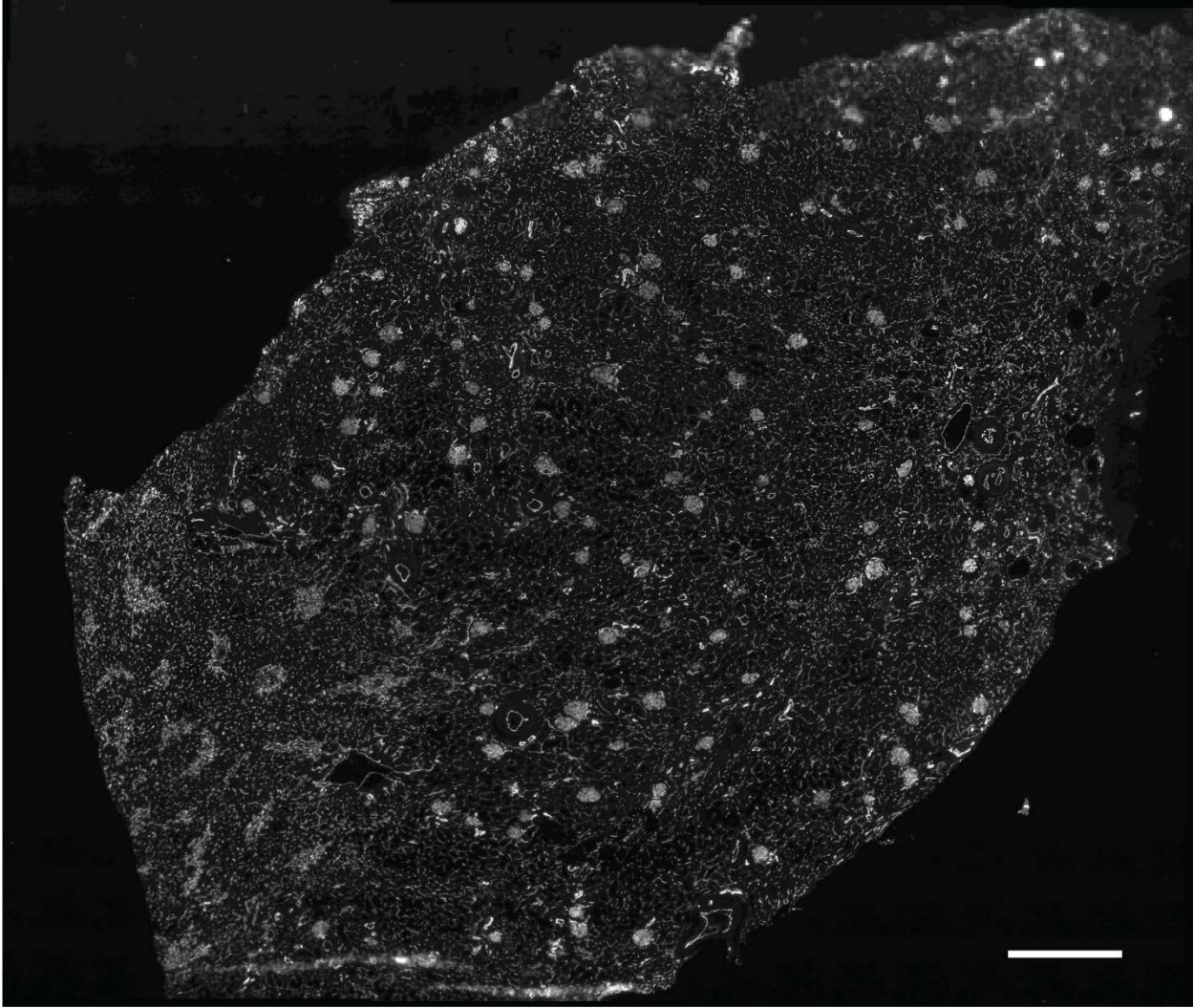


Figure S15: Single channel image of CD31. Scale bar is 1 mm.

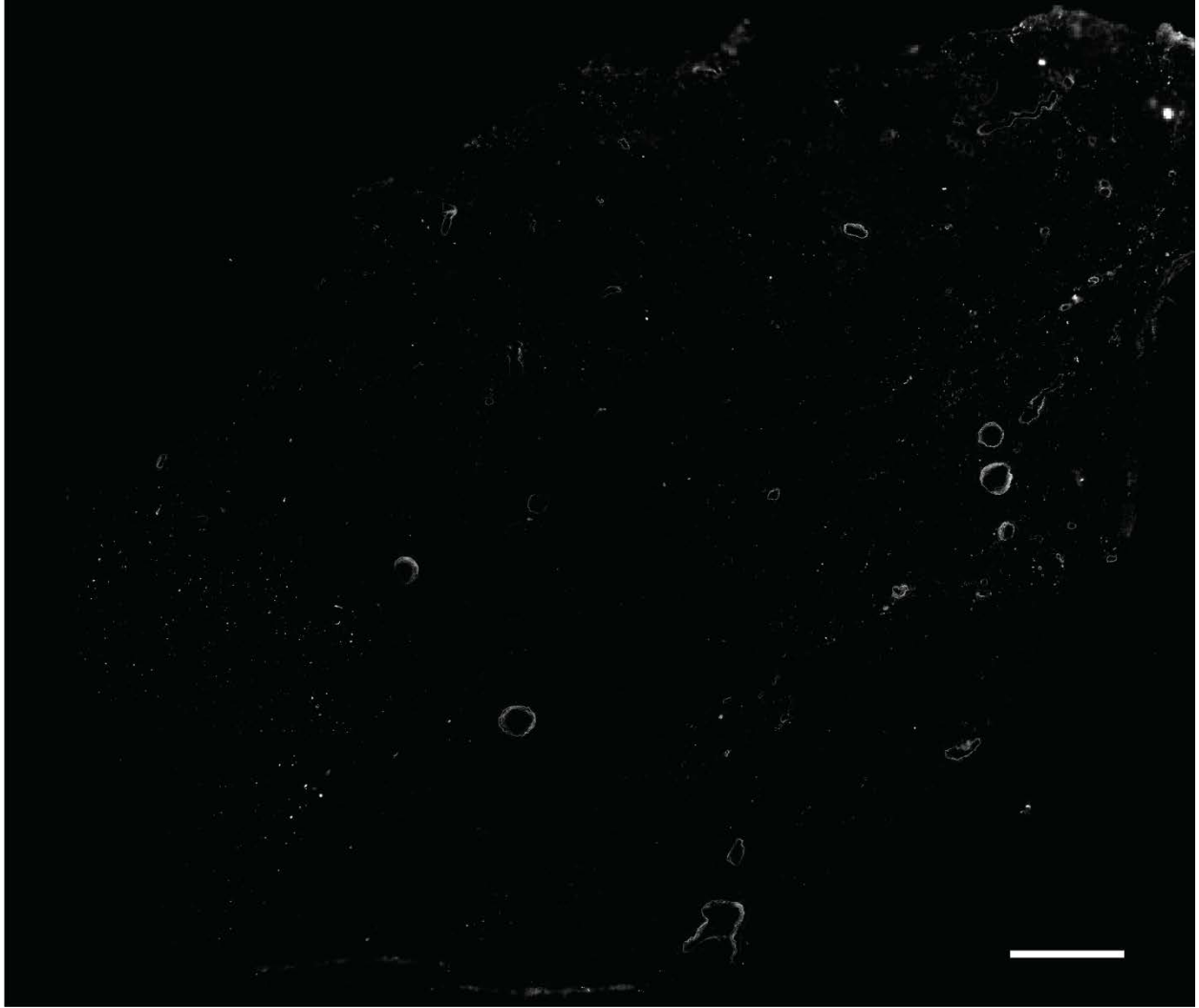


Figure S16: Single channel image of CD38. Scale bar is 1 mm.

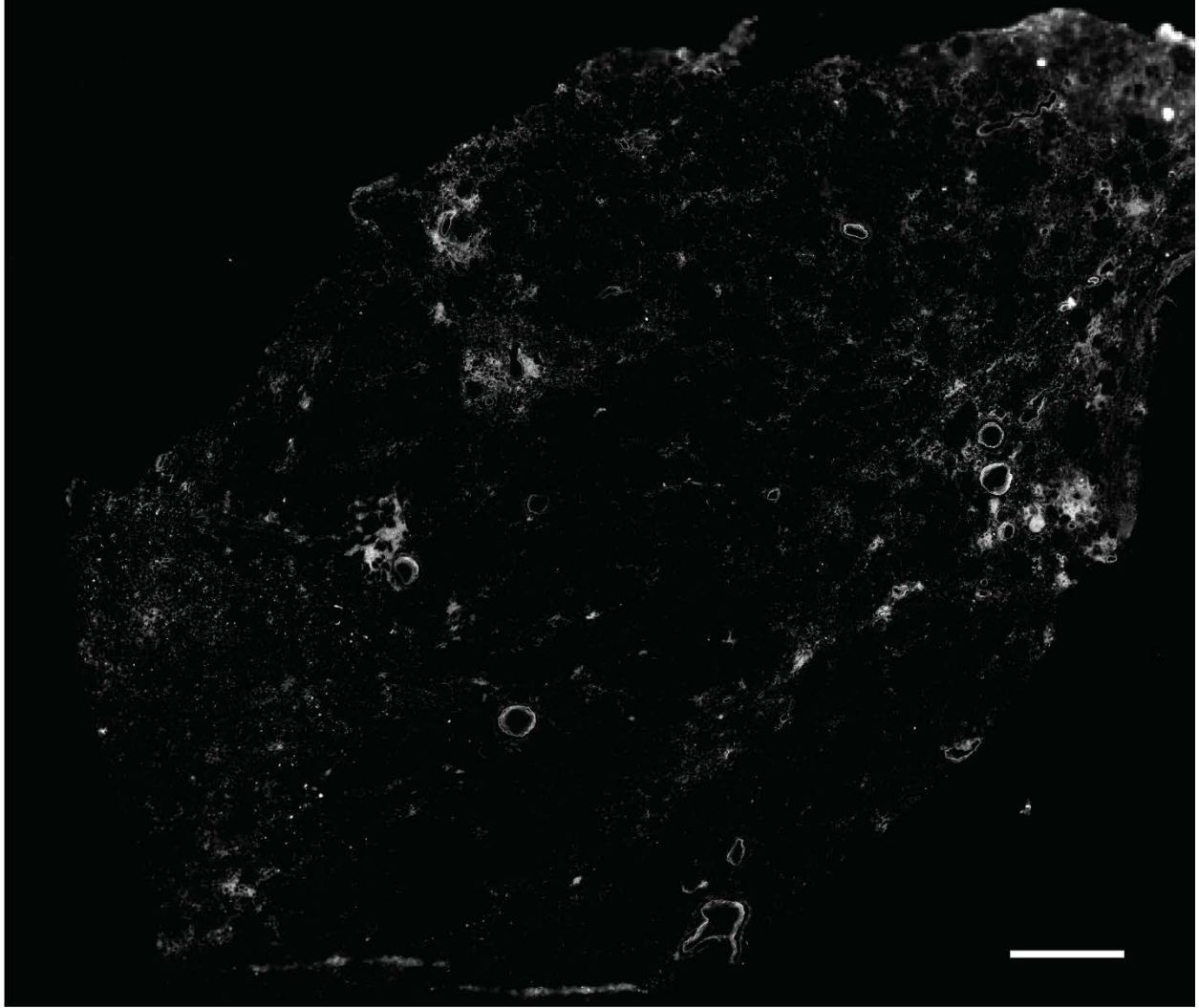


Figure S17: Single channel image of CD45. Scale bar is 1 mm.

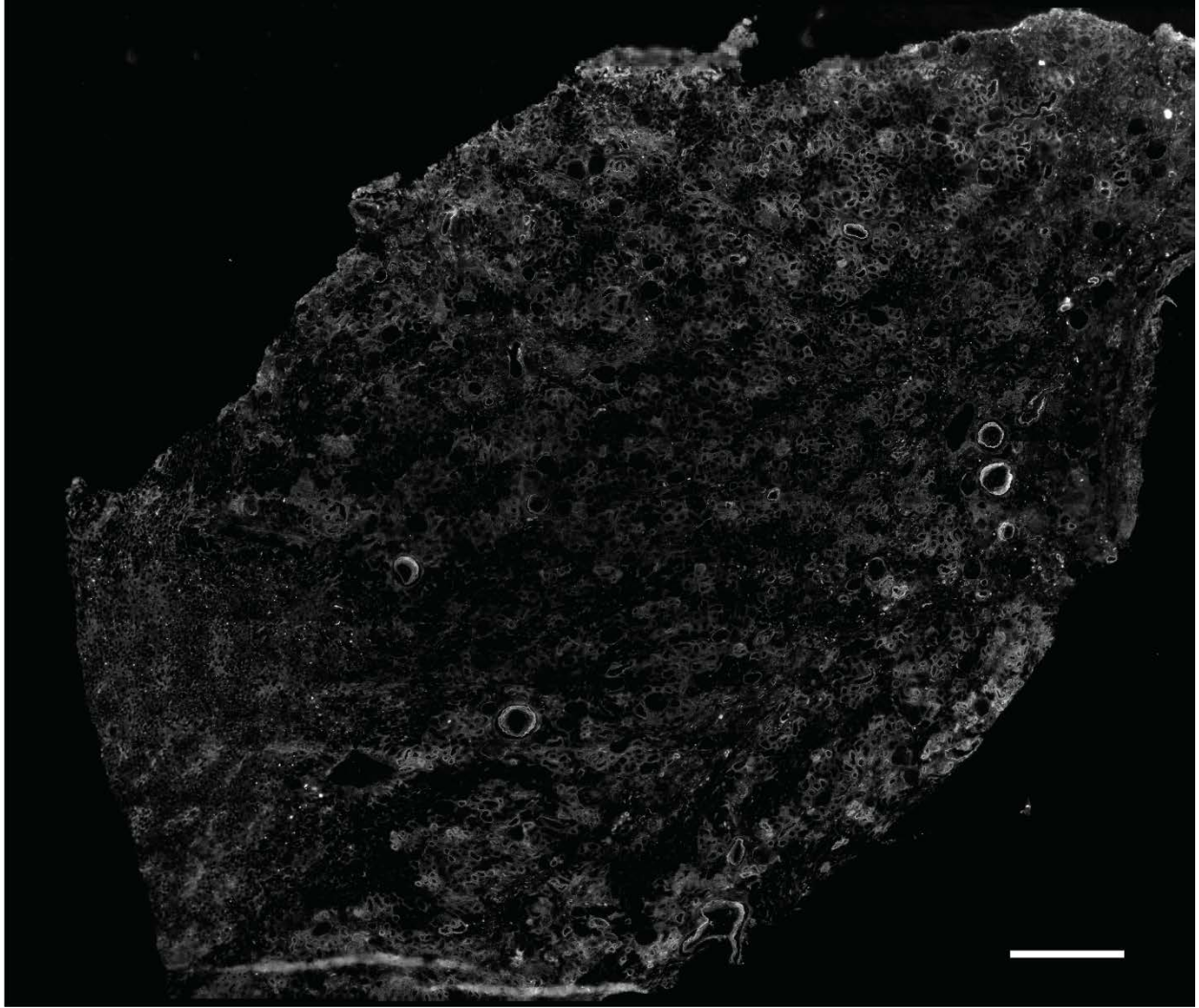


Figure S18: Single channel image of CD90. Scale bar is 1 mm.

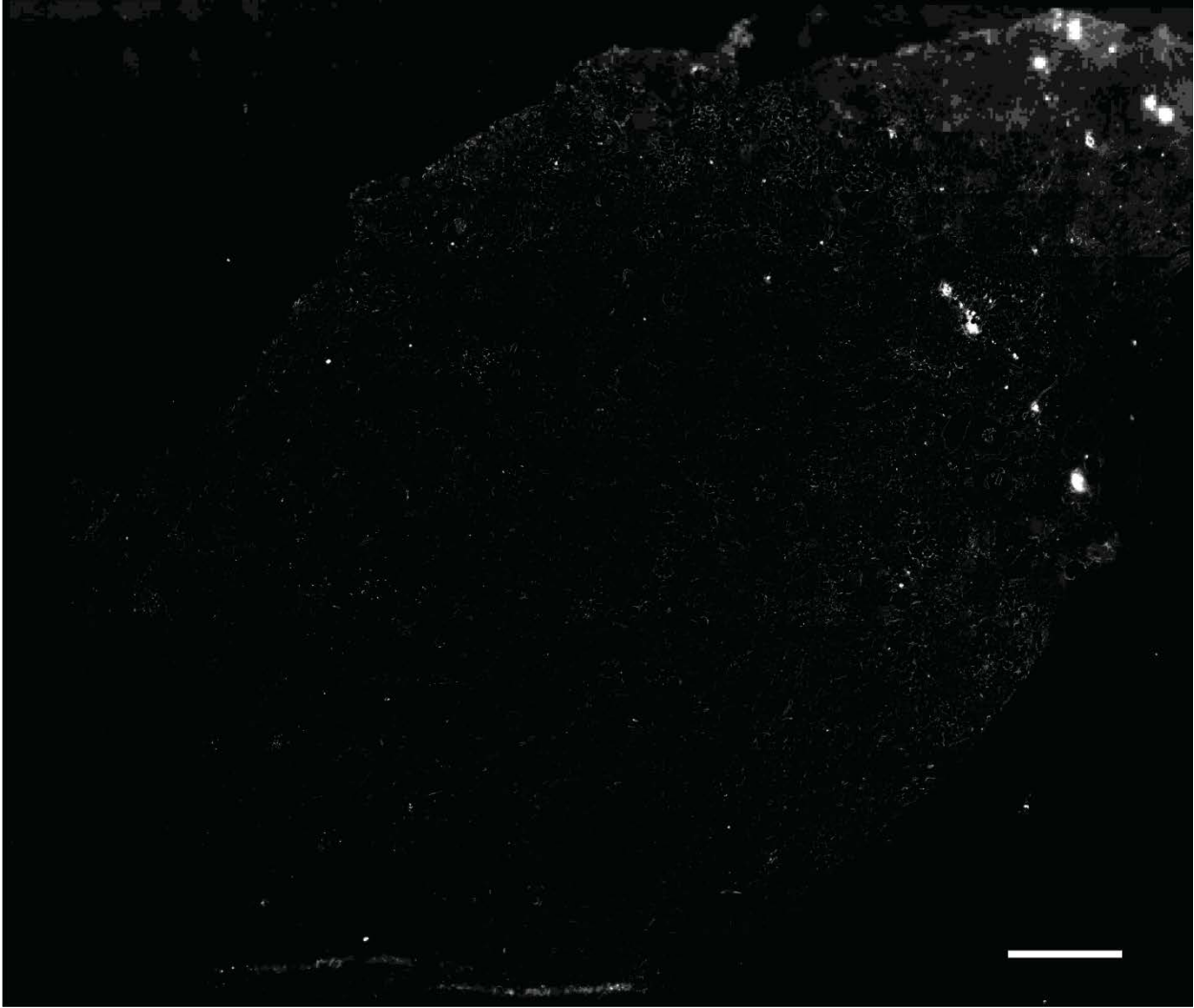


Figure S19: Single channel image of CD93. Scale bar is 1 mm.

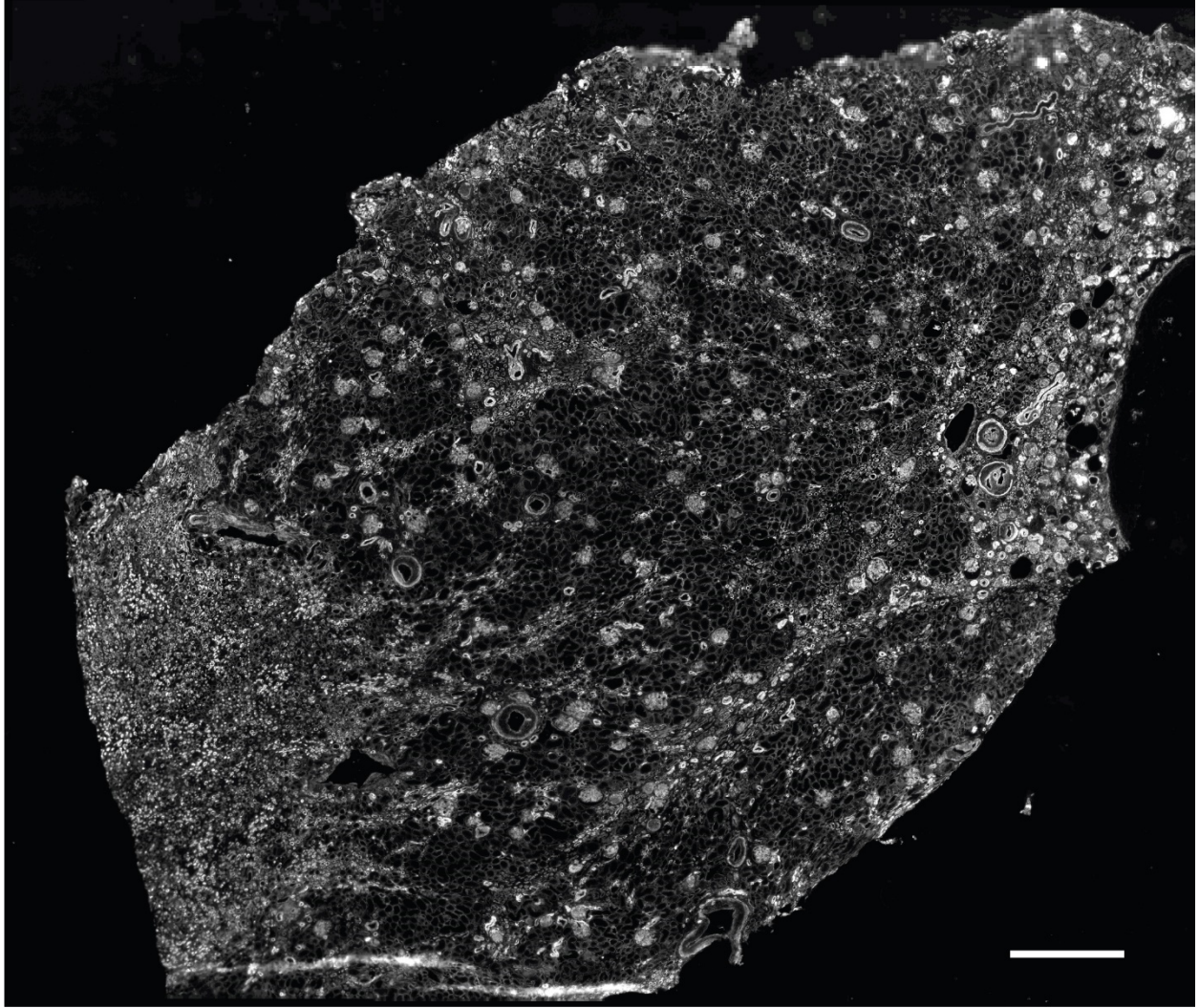


Figure S20: Single channel image of cytokine 7. Scale bar is 1 mm.

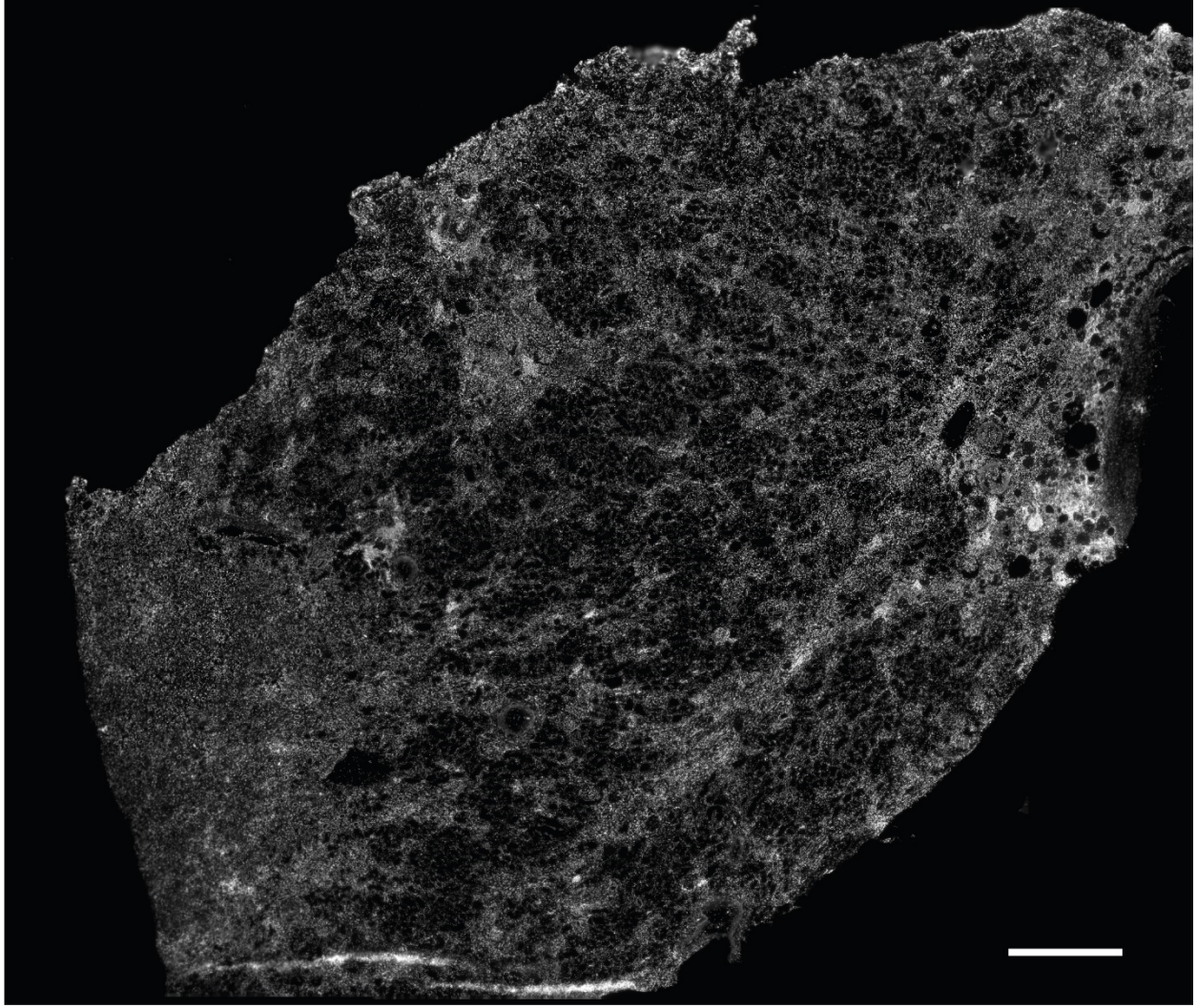


Figure S21: Single channel image of DAPI. Scale bar is 1 mm.

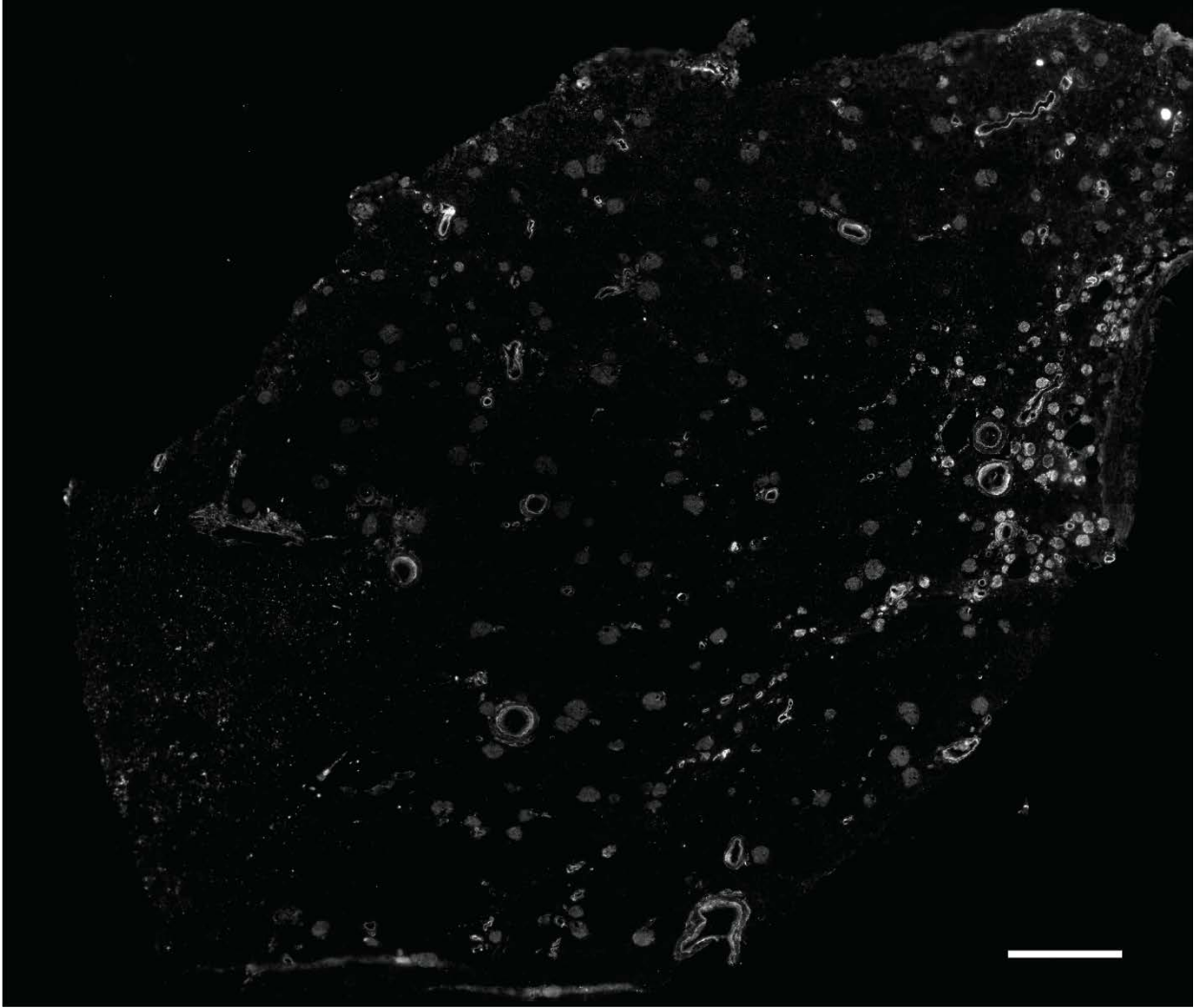


Figure S22: Single channel image of e-cadherin. Scale bar is 1 mm.

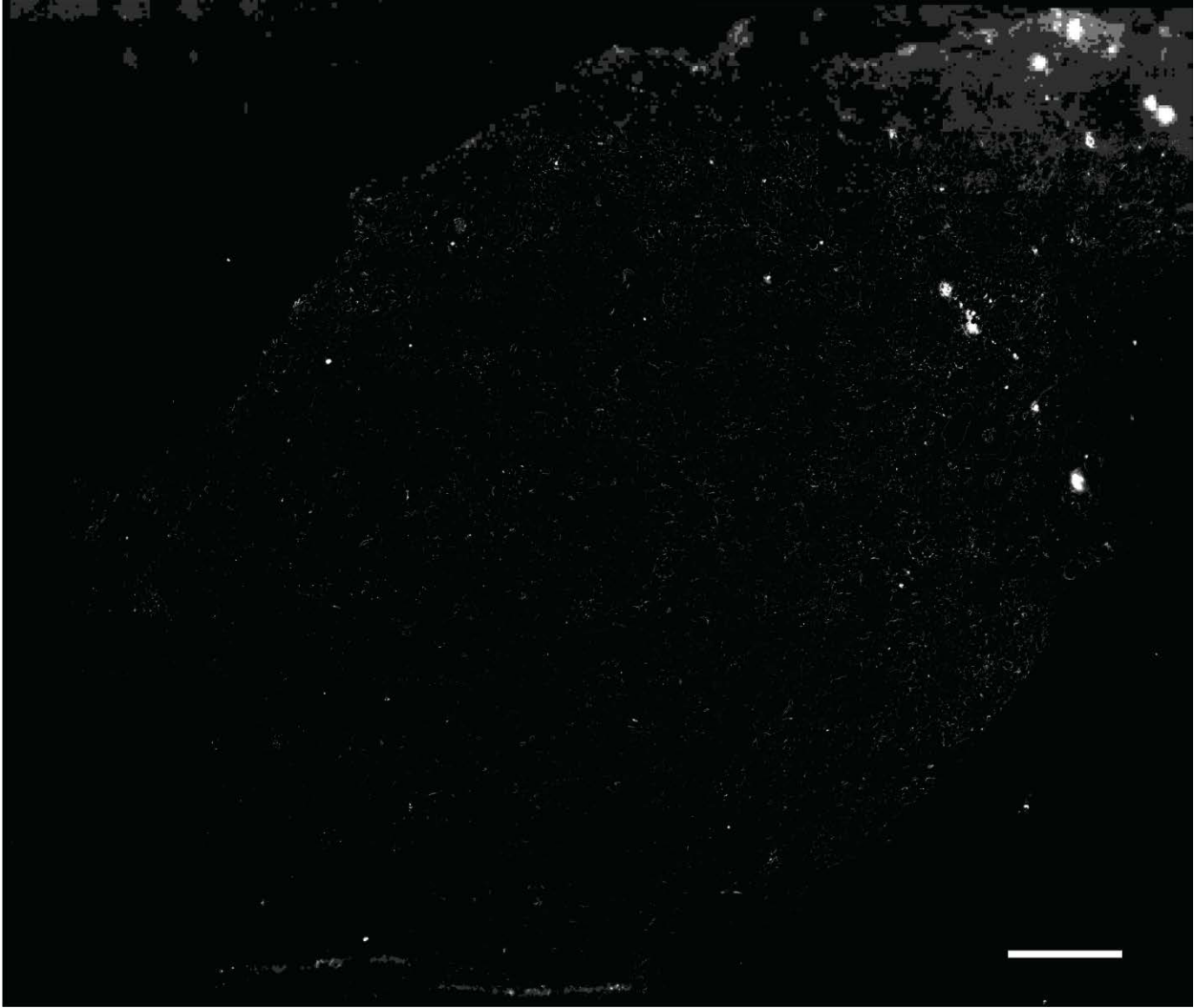


Figure S23: Single channel image of KDR/VEGF. Scale bar is 1 mm.

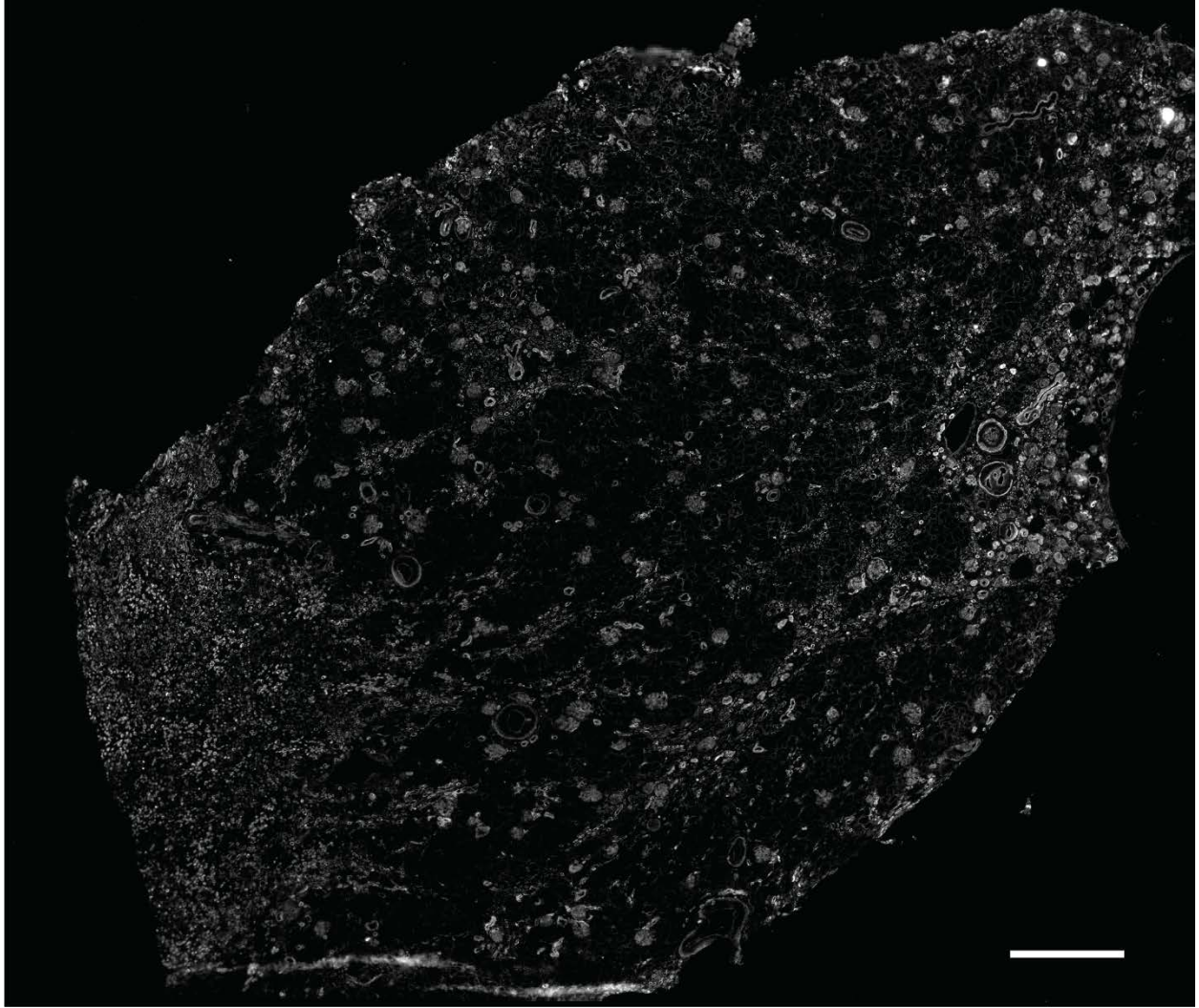


Figure S24: Single channel image of laminin. Scale bar is 1 mm.

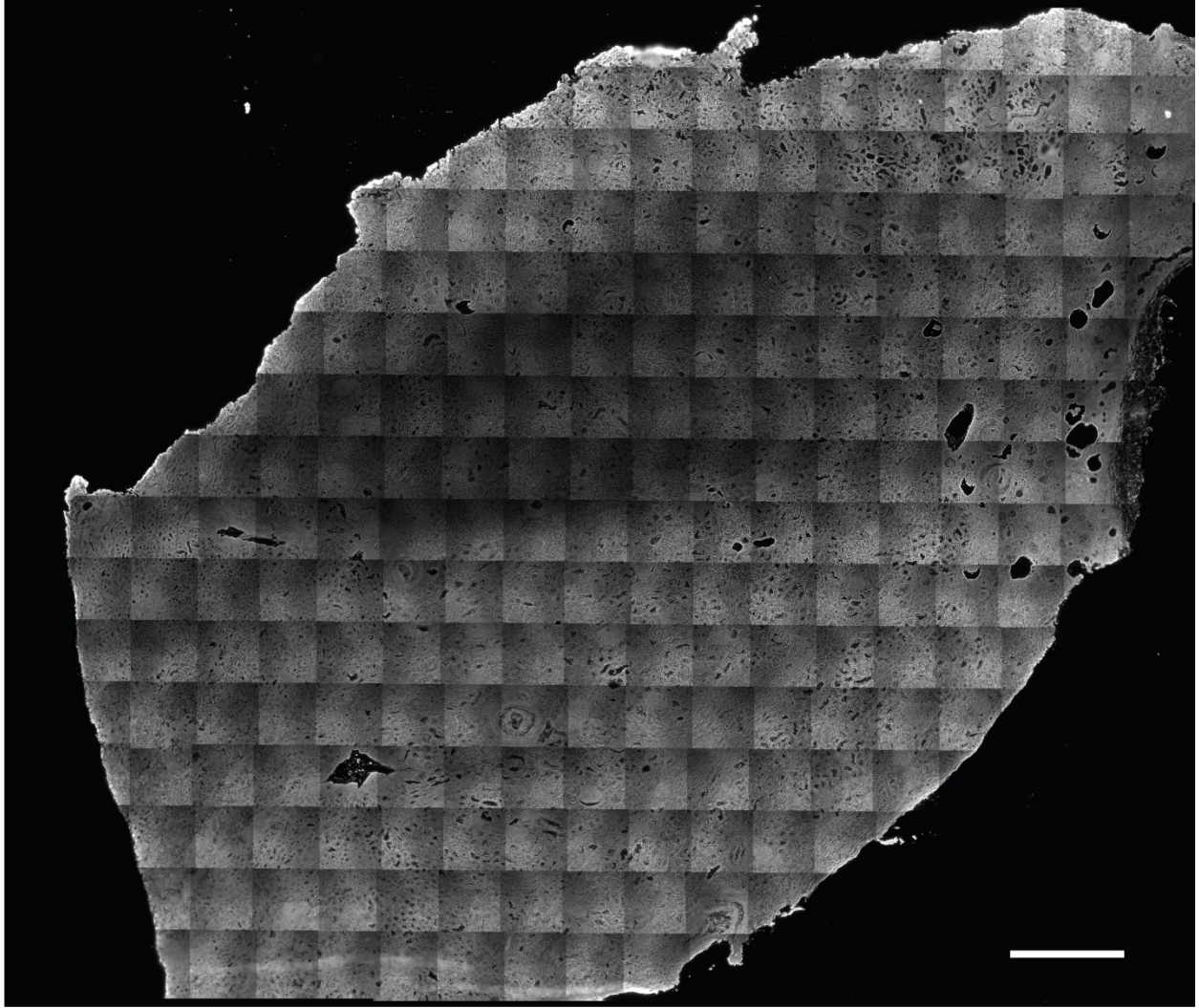


Figure S25: Single channel image of MARCKS. Scale bar is 1 mm.

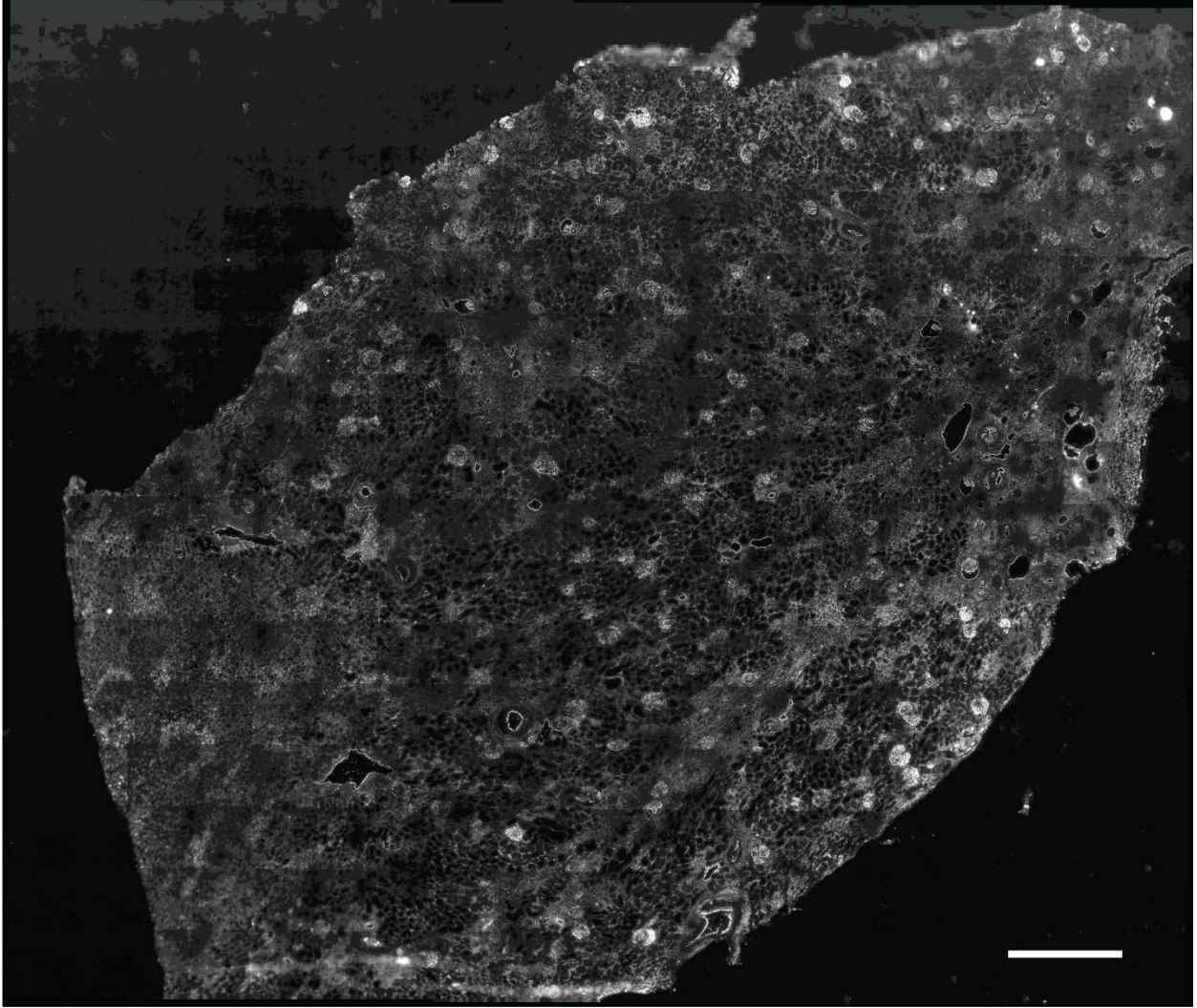


Figure S26: Single channel image of nestin. Scale bar is 1 mm.

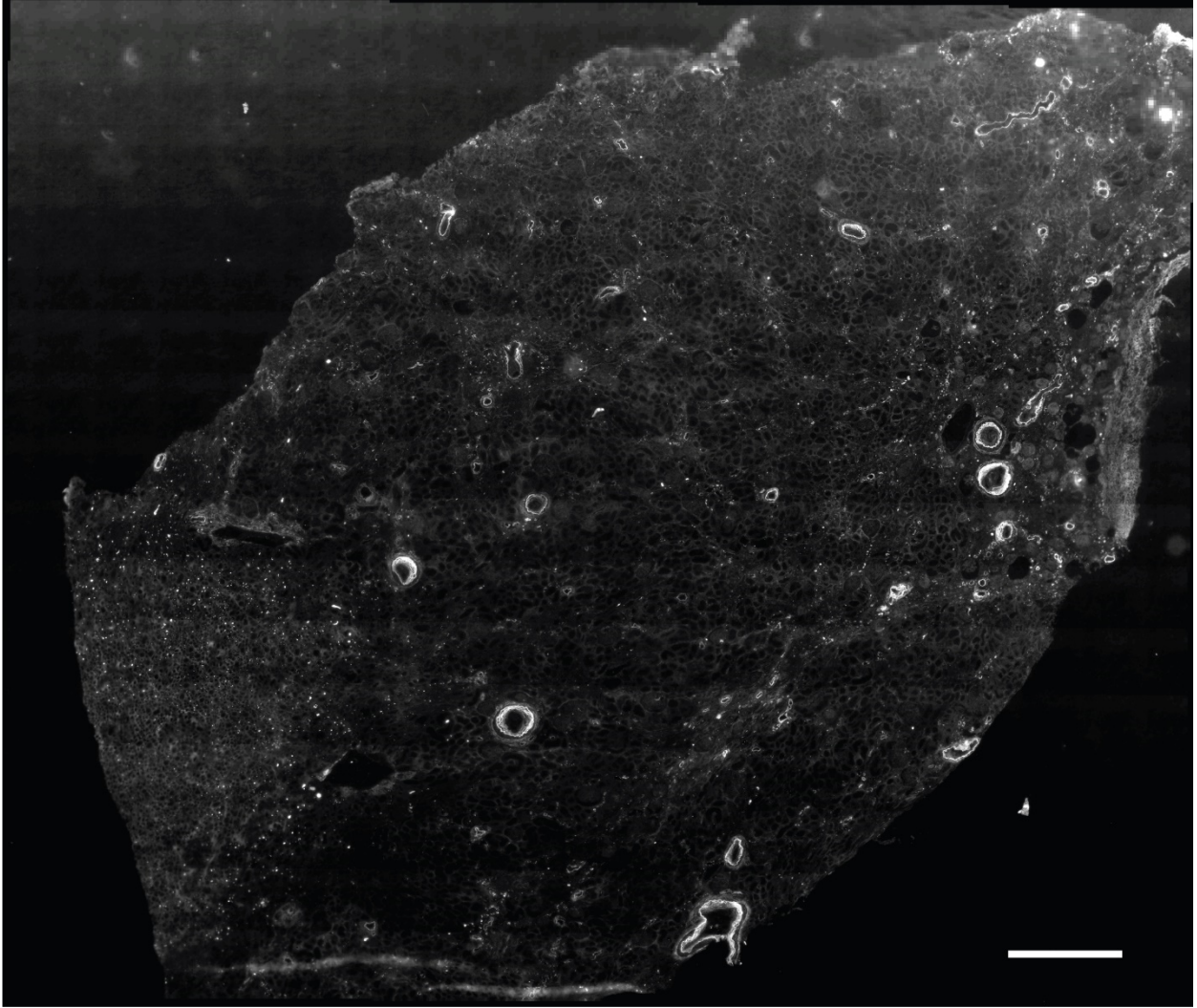


Figure S27: Single channel image of PARP1. Scale bar is 1 mm.

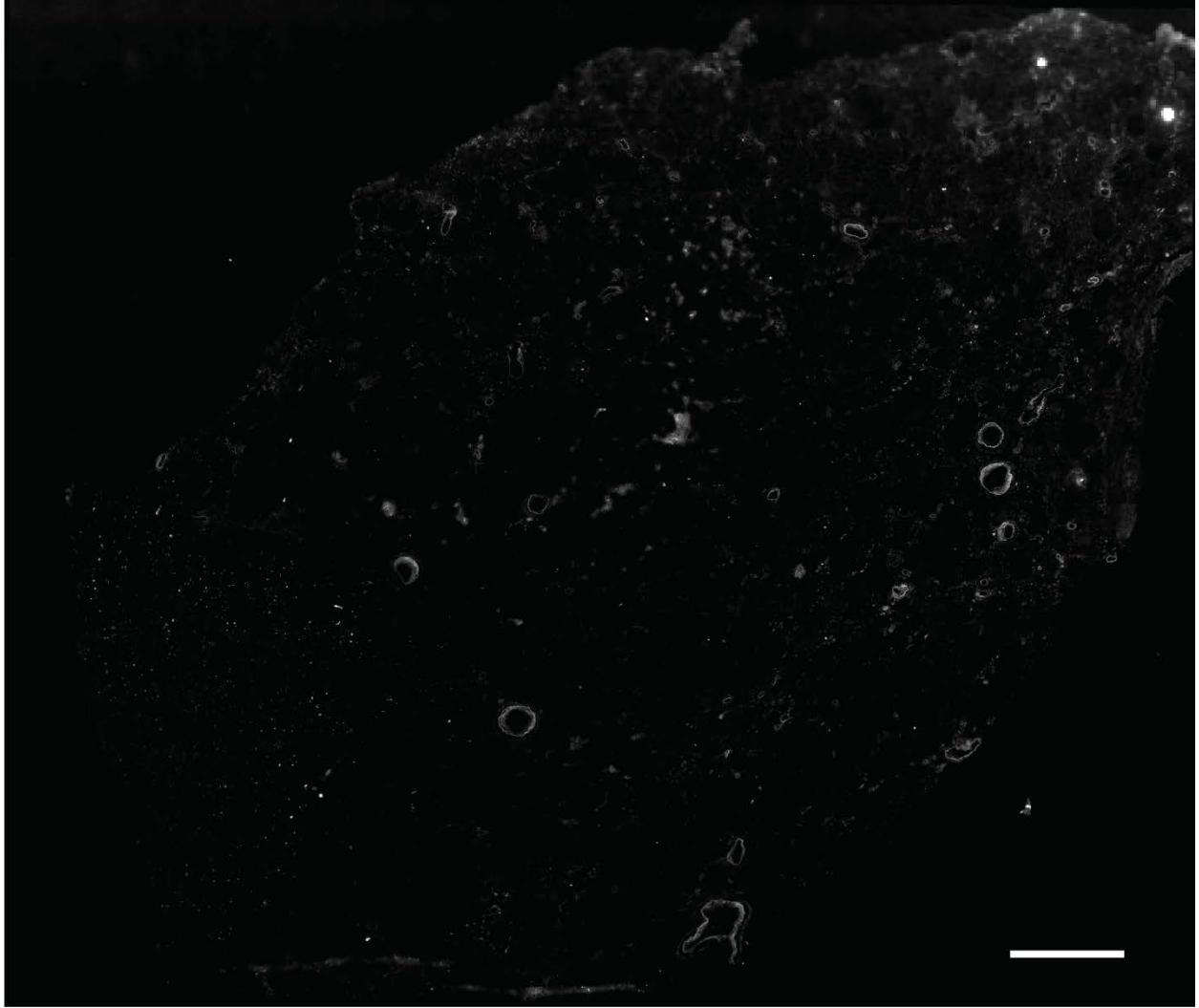


Figure S28: Single channel image of renin. Scale bar is 1 mm.

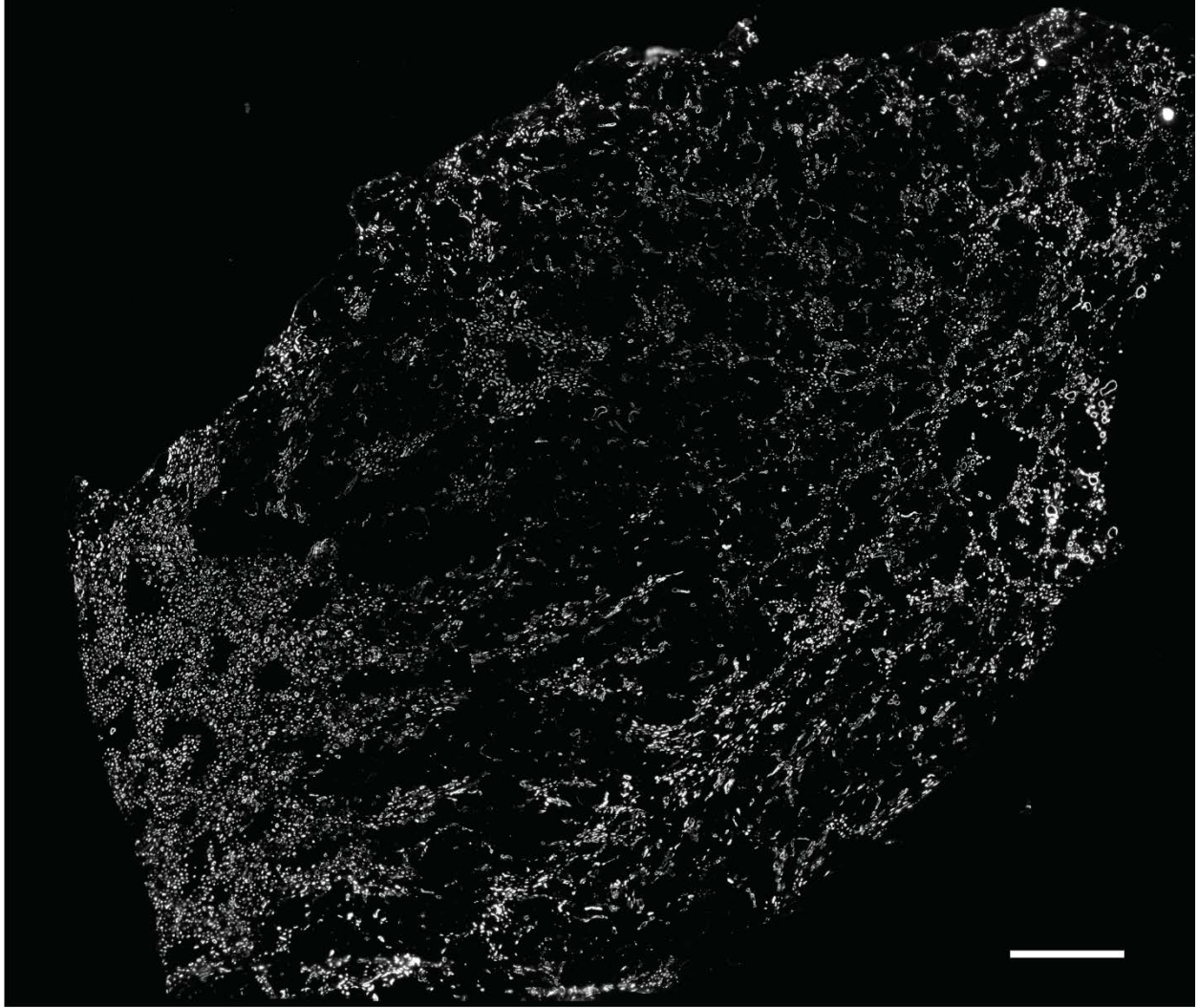


Figure S29: Single channel image of tryptase. Scale bar is 1 mm.

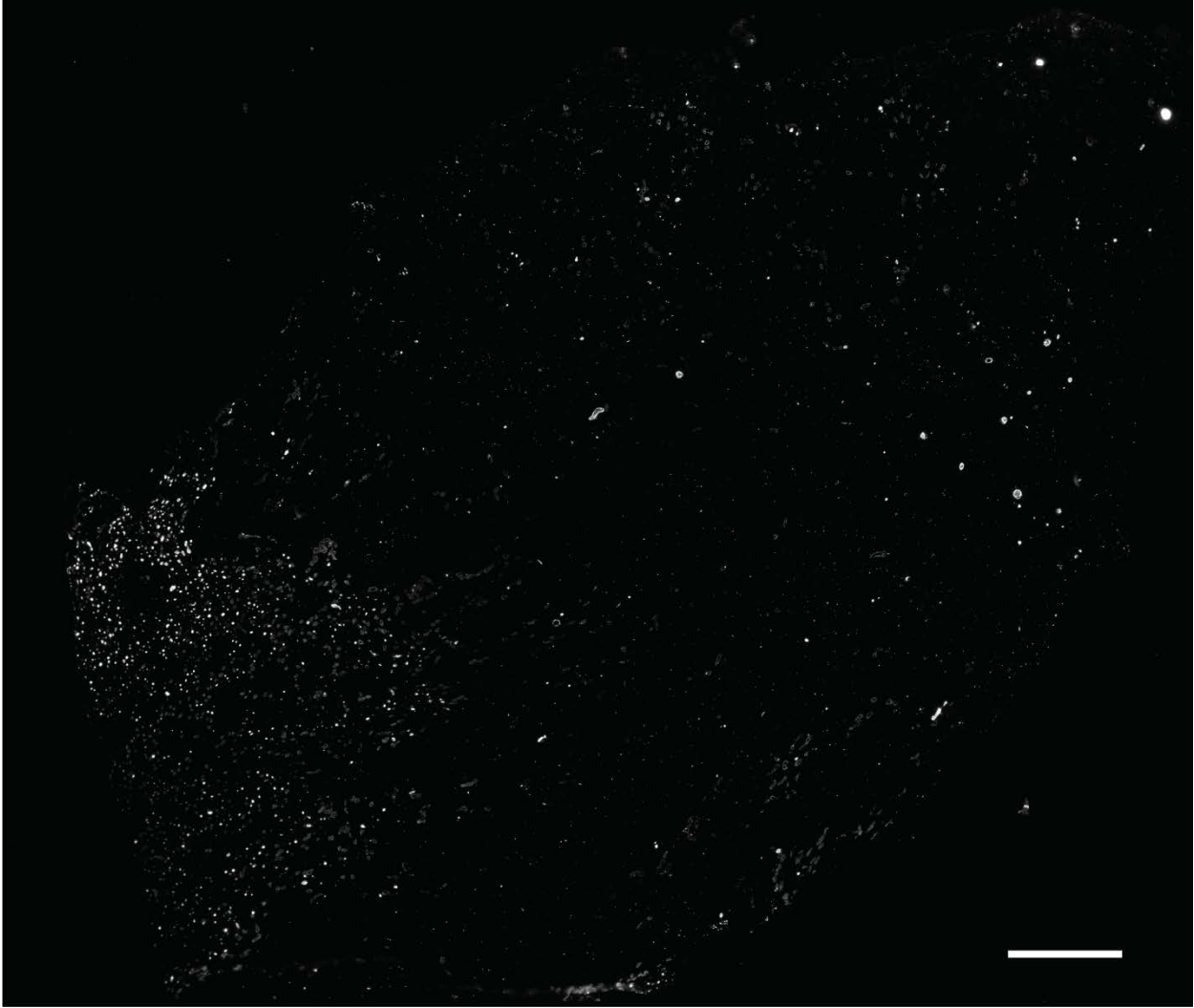


Figure S30: Single channel image of uromodulin. Scale bar is 1 mm.

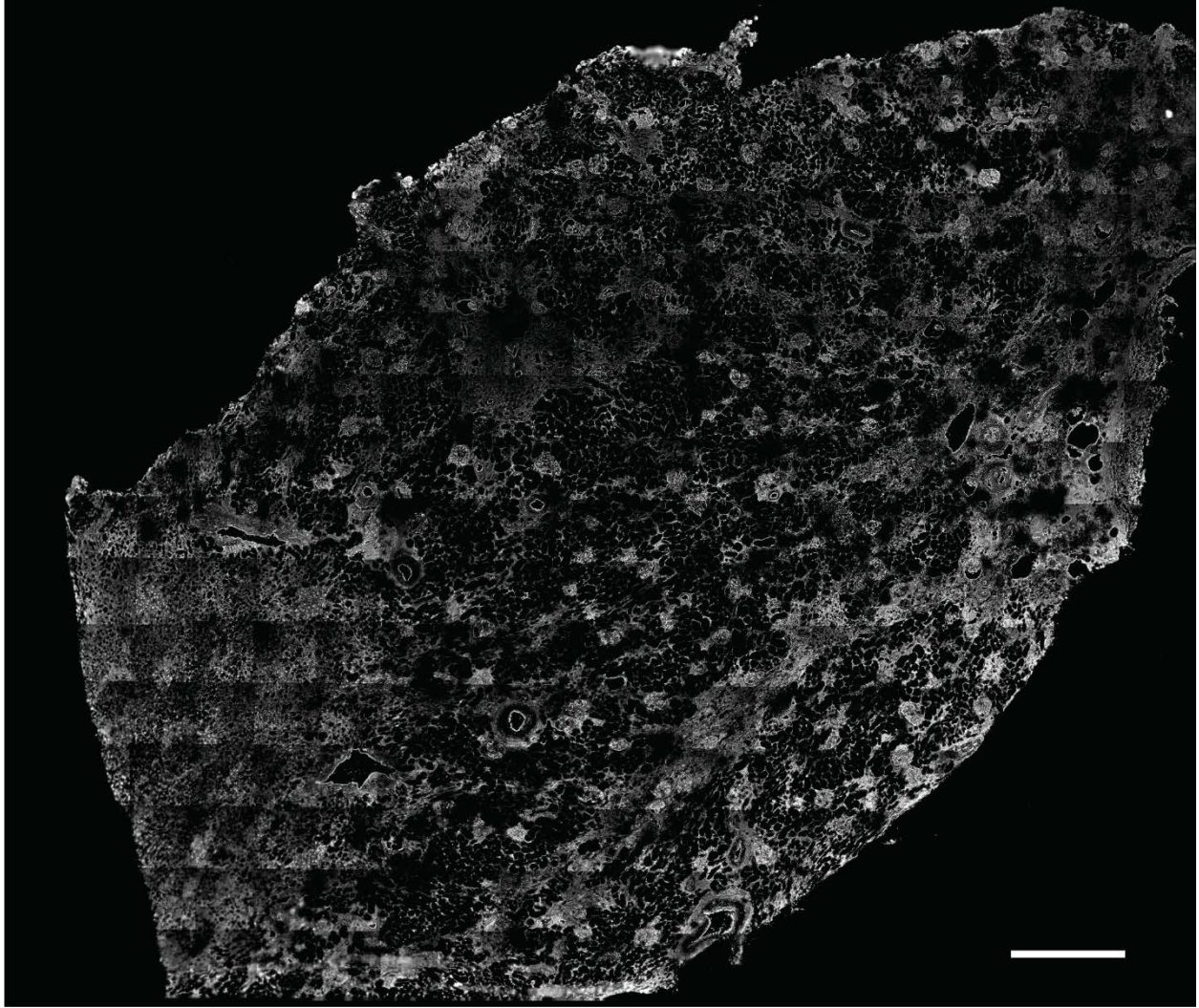


Figure S31: Single channel image of vimentin. Scale bar is 1 mm.

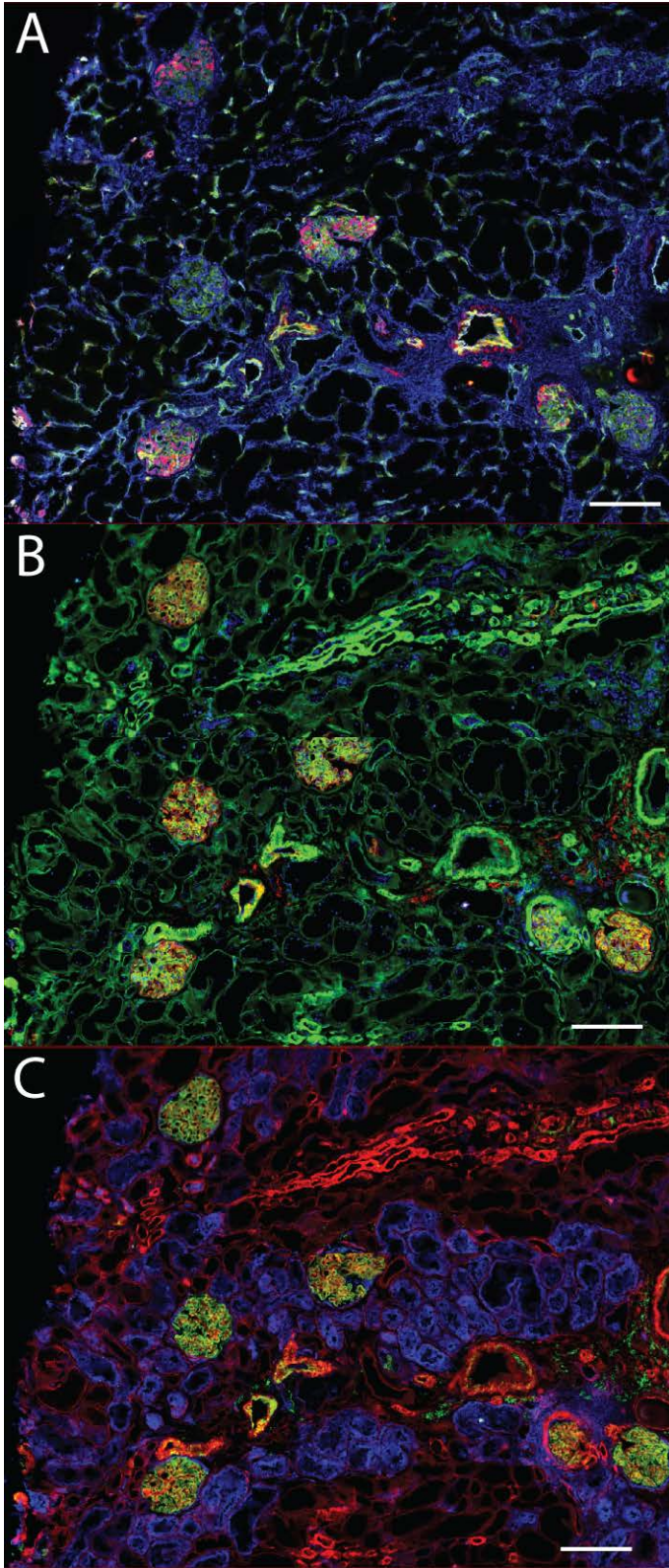


Figure S32: CODEX multiplexed immunofluorescence visualization of glomeruli, using **A)** nestin (red), vimentin (blue), CD31 (green) **B)** PARP1 (blue), e-cadherin (red), laminin (green), and **C)** calbindin (green), cytokeratin 7 (red), CD90 (blue). Scale bars are 200 μm .

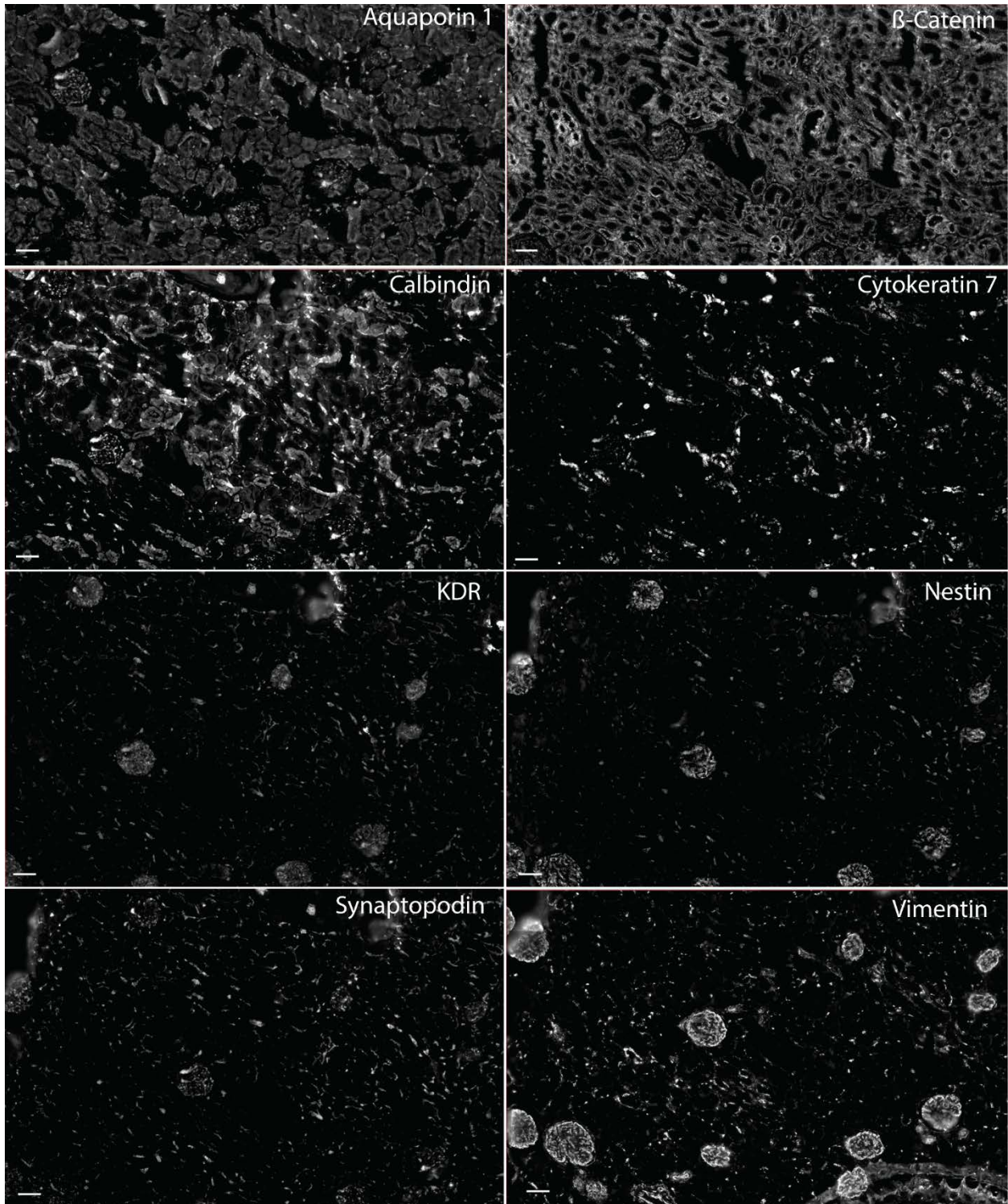


Figure S33: Fluorescence images of antibodies that appropriately stained human FFPE kidney tissue. Scale bars are 100 μ m.

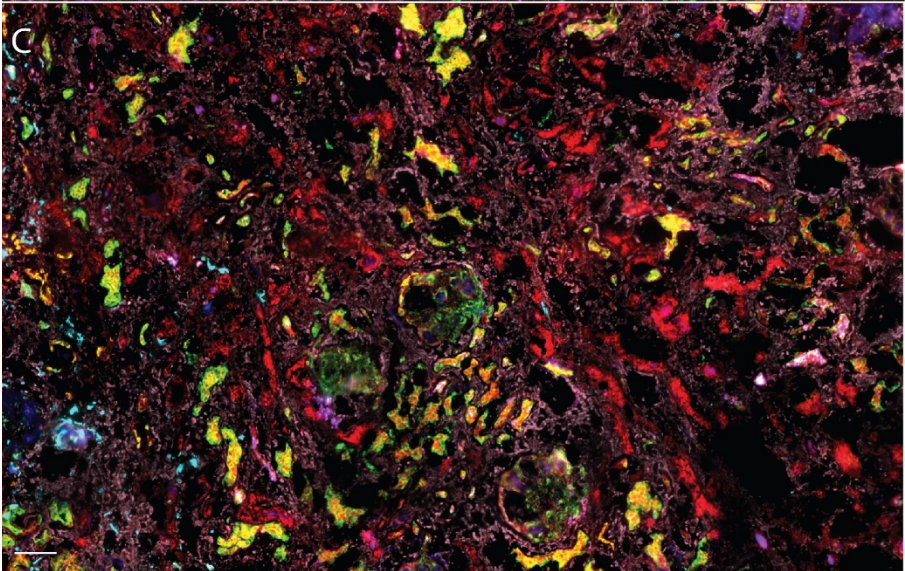
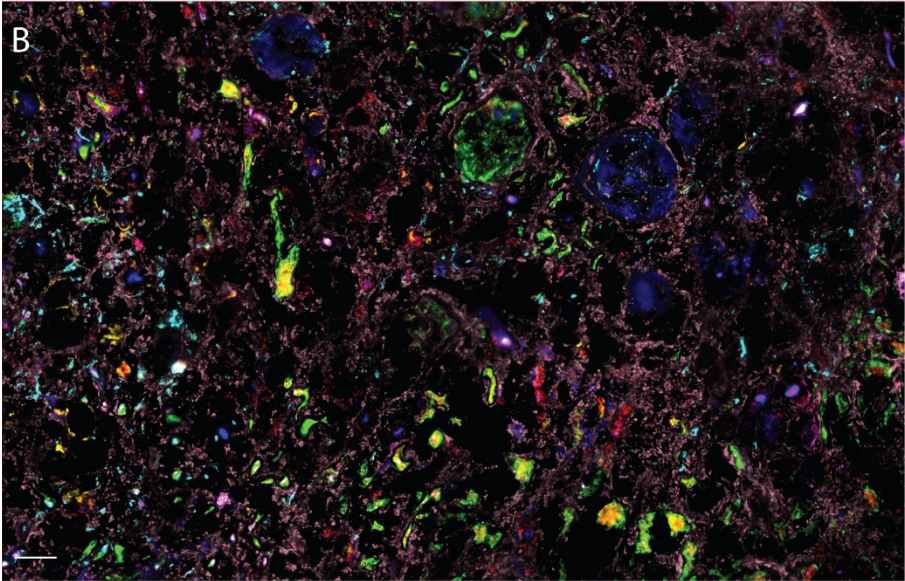
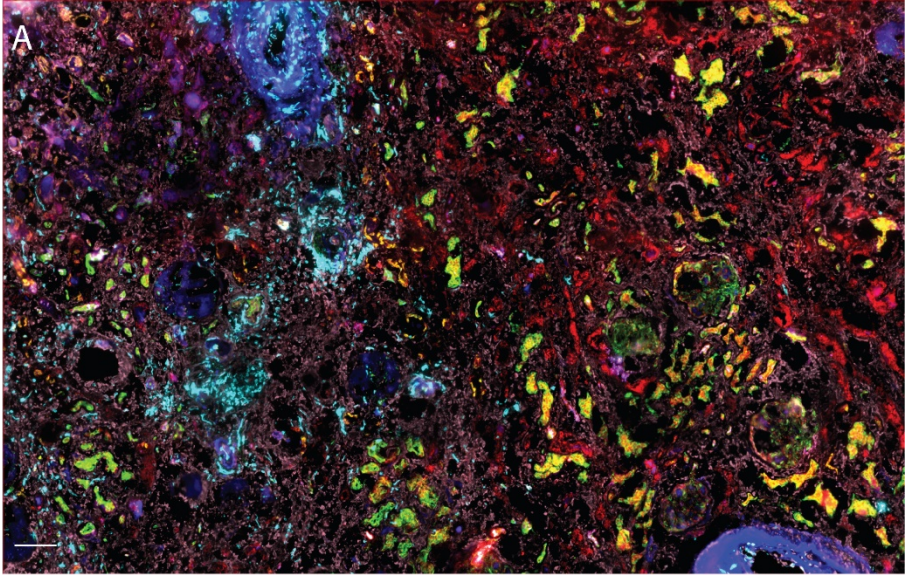


Figure S34: CODEX multiplexed immunofluorescence of kidney section from a 75-year-old female with diabetic nephropathy using CD34 (light green), vimentin (red), PARP1 (dark blue), CD93 (teal), cytokeratin 7 (pink), tryptase (yellow), and MARCKS (peach). Scale bars are 100 μm .

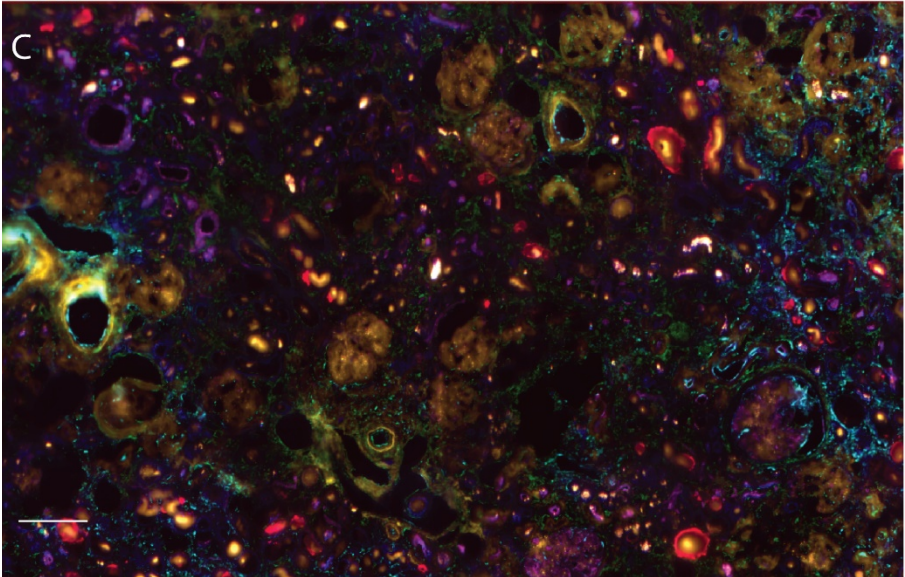
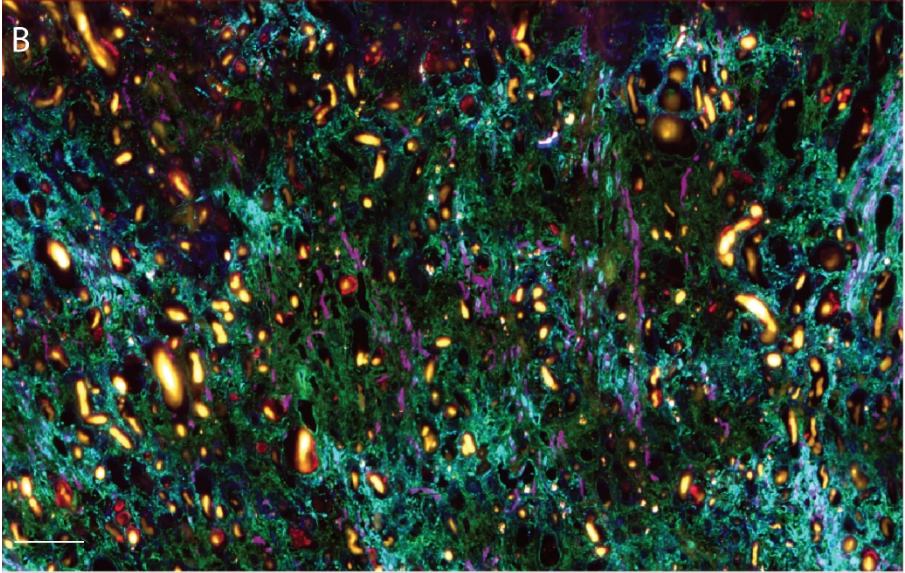
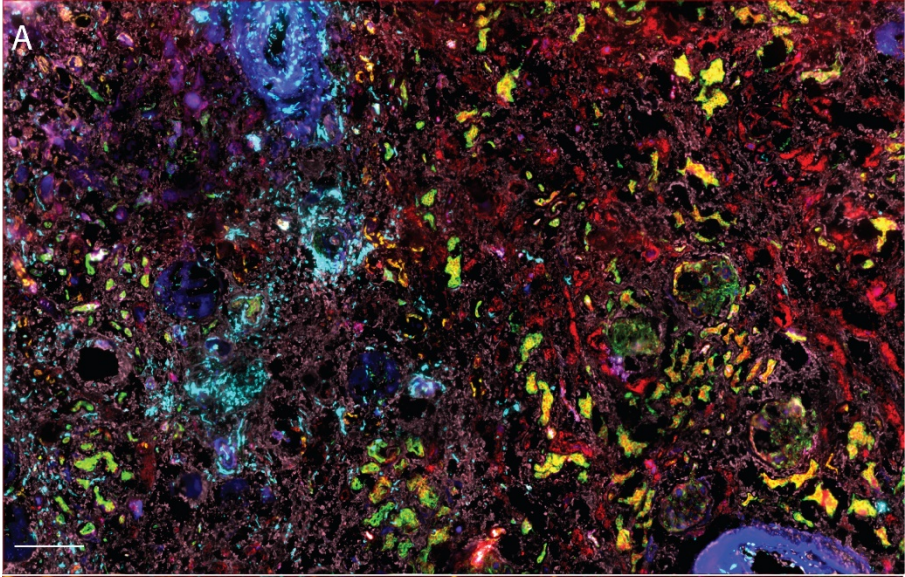


Figure S35: CODEX multiplexed immunofluorescence of kidney section from a 52-year-old male with diabetic nephropathy using AQP1 (purple), CD90 (yellow), synaptopodin (red), β -catenin (teal), vimentin (teal), and α -smooth muscle actin (green). Scale bars are 200 μ m.

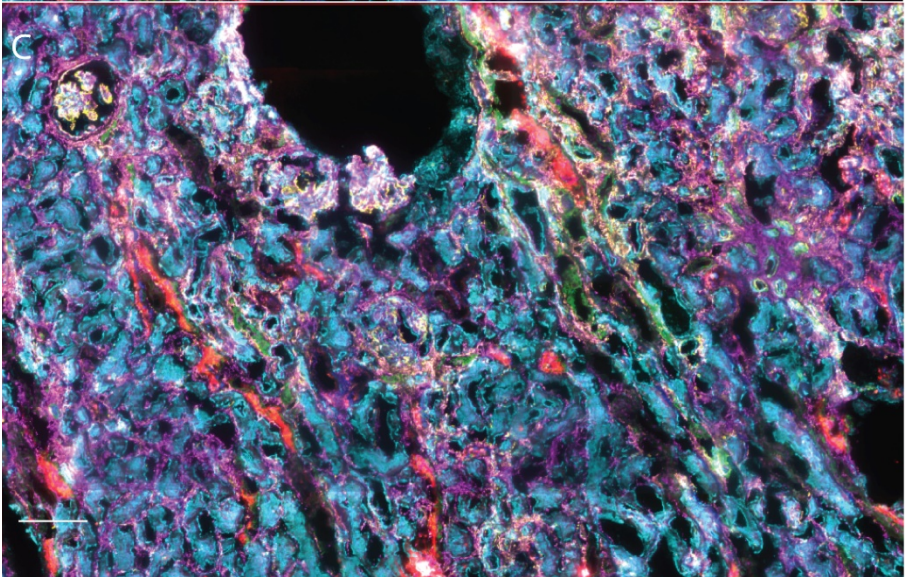
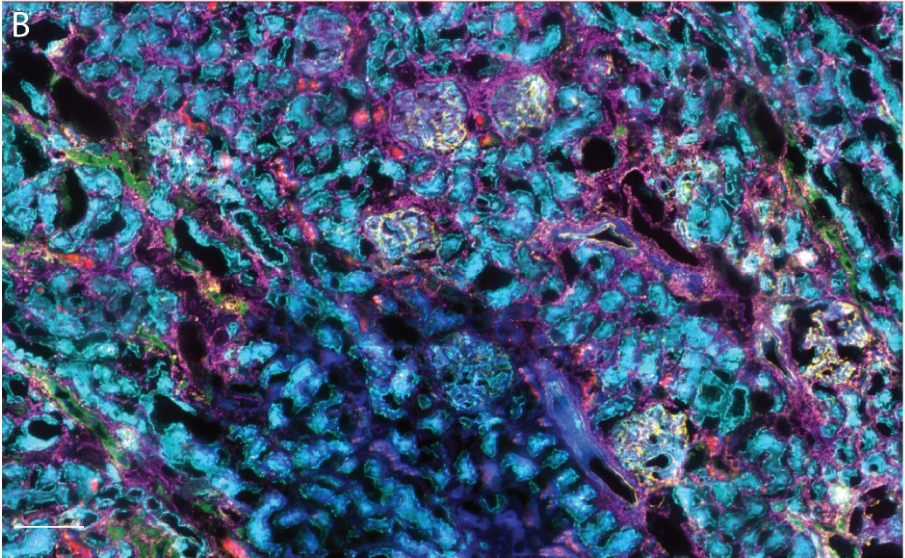
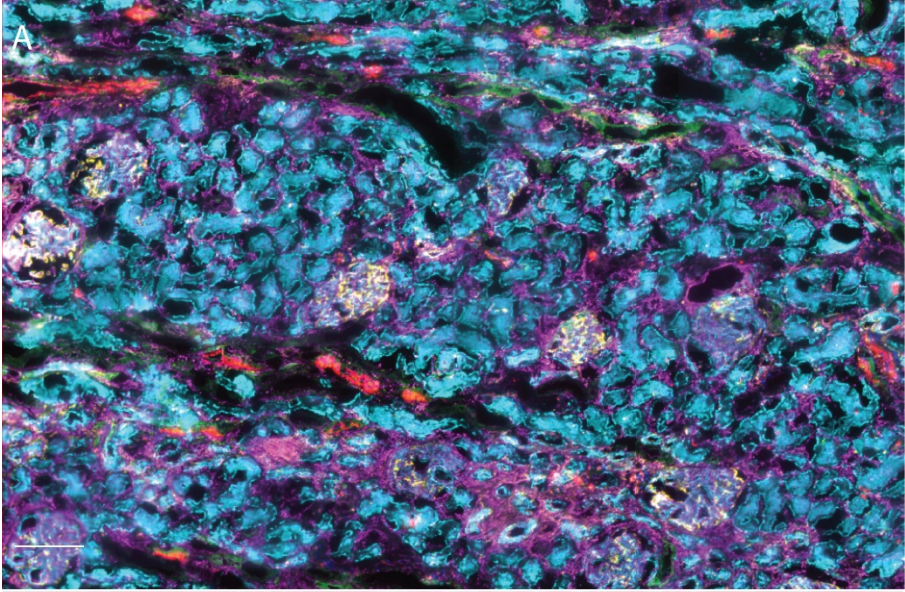


Figure S36: CODEX multiplexed immunofluorescence of kidney section from a 65-year-old male with diabetic nephropathy using aquaporin 1 (teal), aquaporin 2 (red), vimentin (yellow), PARP1 (blue), cytokeratin 7 (green), and α -smooth muscle actin (pink). Scale bars are 200 μ m.

Extended Methods:**Materials:**

HPLC-grade acetone, isopentane, and methanol were purchased from Fisher Scientific (Pittsburgh, PA, USA).

Sample Preparation:

Human kidney tissue was surgically removed during a full nephrectomy and remnant tissue was processed for research purposes by the Cooperative Human Tissue Network at Vanderbilt University Medical Center. Remnant biospecimens were collected in compliance with the Cooperative Human Tissue Network standard protocols and National Cancer Institute's Best Practices for the procurement of remnant surgical research material. Participants were consented for remnant tissue collection in accordance to institutional IRB policies. The excised tissue was flash frozen over an isopentane-dry ice slurry, embedded in carboxymethylcellulose, and stored at -80 °C until use. Kidney tissues were cryosectioned to a 10 µm thickness and thaw mounted onto poly-L-lysine coated glass cover slips and stored at -80 °C until analyzed. A portion of excised tissue was formalin fixed and paraffin embedded (FFPE) for comparison with fresh frozen tissue. FFPE tissue was sectioned to a 10 µm thickness and mounted onto a poly-L-lysine coated glass cover slip.

Frozen tissues were returned to ~20 °C within a vacuum desiccator before being prepared according to the manufacturer's protocols (Akoya Biosciences, Marlborough, MA). In brief, antigen retrieval was performed using a 5 min incubation in acetone. Tissues were then rehydrated in hydration buffer (Akoya Biosciences) and fixed for 10 minutes in a 1.6% paraformaldehyde (Thermo Fischer Scientific, Waltham, MA) solution diluted in hydration buffer. Tissues were incubated in staining buffer (Akoya Biosciences) for 30 min. Tissues were then incubated with blocking buffer (Akoya Biosciences) and primary antibody cocktail (1:200 antibody dilution) for 3 hr within a humidity chamber at ~20 °C. The samples were rinsed with staining buffer before being fixed in a 1.6% paraformaldehyde solution diluted in storage buffer (Akoya Biosciences) for 10 min. The samples were then rinsed in phosphate buffered saline (PBS), incubated for 5 min in cold methanol (~4 °C), and rinsed again in PBS. Samples were then fixed with fixative solution (Akoya Biosciences) before being stored in storage buffer at ~4 °C until used. It is key to note that all nuclease free water was used to prepare all buffers that were not purchased directly from the manufacturer. Similar protocols were used to prepare FFPE tissue with notable exceptions. Unless otherwise specified, the protocols from the manufacturer were used. In brief, tissue was deparaffinized in xylenes (two, 5 min washes) and graded ethanol (100%, 90%, 70%, 50%, and 30% ethanol in water) for 5 min each wash. Antigen retrieval was performed in a pressure cooking using 0.01 M citrate buffer. Tissue was left under pressure for 20 min and then returned to room temperature before incubation in hydration buffer. The remainder of the procedure is the same as with fresh frozen tissue. While some antibody clones can successfully stain both fresh frozen and FFPE tissue, this is not often the case. Here, eight antibodies successfully could stain both fresh frozen and FFPE tissue (SI Figure 35), although other clones may work on FFPE tissue.

Antibody Conjugation:

Pre-conjugated CODEX antibodies were purchased from Akoya Biosciences. Unconjugated primary antibodies were purchased from Abcam (Cambridge, MA) unless otherwise specified. Purified primary antibodies were purchased without any additives or preservatives, many of which prevent successful

antibody conjugation. Antibodies were conjugated and prepared according to the manufacturer's protocols (Akoya Biosciences) with slight deviations. In brief, 50 kDa molecular weight cut off filters were blocked using 500 μ L of a proprietary filter blocking solution (Akoya Biosciences). 50 μ g of each antibody were diluted to 100 μ L of PBS and filtered. Antibodies were reduced with the reduction mixture (Akoya Biosciences) for a maximum of 25 min at \sim 20 $^{\circ}$ C (compared to 30 minutes). The reduction solution was removed by centrifugation (12,000 g) and exchanged with buffer solution (Akoya Biosciences). Each oligonucleotide barcode is rehydrated in 10 μ L nuclease free water (Ambion Inc., Austin, TX) and further diluted in 210 μ L of conjugation solution (Akoya Biosciences). Respective barcodes are added to the reduced primary antibodies and incubated for 2 hr at \sim 20 $^{\circ}$ C. 5 μ L of this conjugated antibody solution is removed for later validation. The solution is then purified by buffer exchanging with purification solution (Akoya Biosciences) and stored in storage solution (Akoya Biosciences) at \sim 4 $^{\circ}$ C until used. After verifying conjugation, the staining profiles of newly conjugated antibodies were compared to a traditional, indirect immunofluorescence experiment. In brief, half of a primary antibody lot was conjugated to an oligonucleotide barcode and half was kept unconjugated. For comparison, unconjugated primary antibody was visualized using traditional indirect IF with a fluorophore that was spectrally resolved from that attached to the corresponding oligonucleotide barcode conjugated antibody. Both sets of primaries were incubated and visualized concurrently to measure overlap between the conjugated and unconjugated antibodies, demonstrating similar selectivity between the two methods.

As discussed in the main text, most of the tested primary antibodies successfully conjugate to oligonucleotide barcodes. There are still uncertainties surrounding successful antibody conjugation and why some clones conjugate well while others do not, but we preferentially conjugate antibodies that were purified from the manufacturer (e.g. without glycerol, azides, BSA, and other additives), recombinant, extensively validated (e.g. knock out validated), and validated for a variety of systems (e.g. mouse, rat, human) and approaches. While most of these criteria should not affect the conjugation chemistry, the extensive commercial testing and purification lends to better and, perhaps, more robust primary antibodies.

CODEX Multiplexed Immunofluorescence:

The recommended antibody concentrations provided by the manufacturer were used in all cases. Antibodies are diluted in reporter solution (Akoya Biosciences) to a 1:200 dilution in sets of three with the addition of 1 μ g of DAPI. The CODEX system automatically dispensed secondary oligonucleotide barcodes automatically. Microscopy was performed on a Zeiss Axio Observer (Carl Zeiss AG, Oberkochen, Germany) using a Colibri 7 LED lightsource (Carl Zeiss) and C13440 camera (Hamamatsu, Shizuoka, Japan). Images were acquired with a 10% tile overlap and a z-stack ranging from 11 to 20 tiles (depending on the tissue size). Images were processed using ZEN (Zeiss). Visualization and cell segmentation was performed using QuPath using the following parameters (8 μ m background radius, 1.5 μ m sigma, 10-100 μ m² allotted nuclear area, 150 intensity threshold, and 10 μ m cell expansion.⁵¹ Signal to background was determined using the initial autofluorescence image as background/noise, so positive signal must be greater than 10 times background signal. Neighborhood analysis was performed using MATLAB and CytoMAP.⁵² In brief, neighborhoods were established 40 μ m from the cell center. Signal was normalized to the max mean fluorescence intensity values and the number of clusters was determined using the Davies Bouldin criteria. Regions were determined using default neural network criteria.

- S1. Bankhead P, Loughrey MB, Fernández JA, et al. **QuPath: Open source software for digital pathology image analysis.** *Scientific Reports.* 2017;**7**:16878.
- S2. Stoltzfus CR, Filipek J, Gern BH, et al. **CytoMAP: A Spatial Analysis Toolbox Reveals Features of Myeloid Cell Organization in Lymphoid Tissues.** *Cell Reports.* 2020;**31**:107523.